JACS
JOURNAL OF THE AMERICAN CHEMICAL SOCIETY
pubs.acs.org/JACS
Article

Open-Shell Early Lanthanide Terminal Imides

Theresa E. Rieser, Renita Thim-Spöring, Dorothea Schädle, Peter Sirsch, Rannveig Litlabø, Karl W. Törnroos, Cäcilia Maichle-Mössmer, and Reiner Anwander*

Cite This: J. Am. Chem. Soc. 2022, 144, 4102–4113
Read Online

ABSTRACT: Group 3- and 4f-element organometallic chemistry and reactivity are decisively driven by the rare-earth-metal/lanthanide (Ln) ion size and associated electronegativity/ionicity/Lewis acidity criteria. For these reasons, the synthesis of terminal "unsupported" imides [Ln=NR] of the smaller, closed-shell Sc(III), Lu(III), Y(III), and increasingly covalent Ce(IV) has involved distinct reaction protocols while derivatives of the "early" large Ln(III) have remained elusive. Herein, we report such terminal imides of open-shell lanthanide cations Ce(III), Nd(III), and Sm(III) according to a new reaction protocol. Lewis-acid-stabilized methylidene complexes [Tp^{tBu,Me}Ln(μ_3-CH$_2$){(μ_2-Me)-MMe$_2$}$_2$] (Ln = Ce, Nd, Sm; M = Al, Ga) react with 2,6-diisopropylaniline (H$_2$NAr^{iPr}) via methane elimination. The formation of arylimide complexes is governed by the Ln(III) size, the Lewis acidity of the group 13 metal alkyl, steric factors, the presence of a donor solvent, and the sterics and acidity (pK_a) of the aromatic amine. Crucially, terminal arylimides [Tp^{tBu,Me}Ln(=NAr^{iPr})(THF)$_2$] (Ln = Ce, Nd, Sm) are formed only for M = Ga, and for M = Al, the Lewis-acid-stabilized imides [Tp^{tBu,Me}Ln(NAr^{iPr})(AlMe$_3$)] (Ln = Ce, Nd, Sm) are persistent. In stark contrast, the [GaMe$_3$]-stabilized imide [Tp^{tBu,Me}Ln(NAr^{iPr})(GaMe$_3$)] (Ln = Nd, Sm) is reversibly formed in noncoordinating solvents.

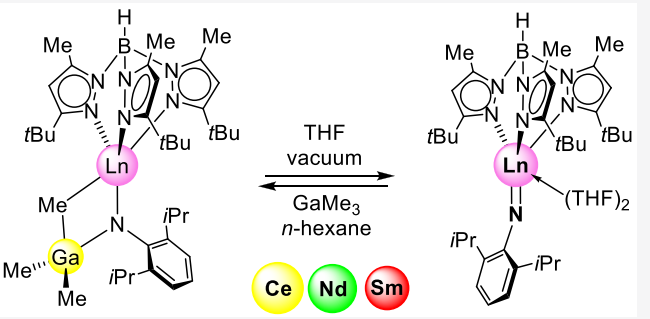

INTRODUCTION

The last two decades have witnessed ever-increasing interest in rare-earth-metal (Ln) complexes featuring multiply bonded (organo)imido ligands.[1−5] Contrary to d-transition metal and 5f-element chemistry,[5−12] the feasibility of terminal "unsupported" (organo)imides [Ln=NR] has posed a major challenge.[1−5] Predominantly ionic bonding situations in rare-earth-metal complexes direct multiply charged, hard monodentate ligands such as [CR$_2$]$^{2-}$[13,14] and [NR]$^{2-}$ in bridging positions.[15,16] On the other hand, kinetic stabilization (via sterically demanding imido ligands) necessitates advanced synthesis protocols.[17] The linking element of most applied syntheses is the use of highly reactive rare-earth-metal alkyl precursors in order to ensure the complete deprotonation of comparatively Brønsted acid aromatic amines and silylamines.[5] Alternatively, the ultimate deprotonation of a [Ln−NHR] moiety can be achieved by an external base (e.g., LiR, LiNR$_2$). Both strategies are prone to metal-capping or bridging imido functionalities.[18−22]

The currently available terminal rare-earth-metal imides are limited to closed-shell (d^0, f^0, f^{14}) derivatives exclusively.[22−28] In 2010, Chen and co-workers isolated the first terminal scandium imide complex [MeC(NAr)CHC(Me)(N(CH$_2$)$_2$-NMe$_2$)Sc(=NAr^{iPr})(DMAP)] (NAr^{iPr}=NC$_6$H$_3$*i*Pr$_2$-2,6) by the reaction of the respective β-diketiminato-based tridentate-ligand-supported scandium dimethyl compound with 2,6-diisopropylaniline and *N*,*N*-dimethyl-4-aminopyridine (DMAP).[23] The X-ray structure analysis, DFT calculations, and intrinsic imido reactivity provided clear and conclusive evidence for the existence of a multiply bonded [Sc=NR] moiety.[3] In the meantime, several terminal organoimides of the smallest and least electropositive rare-earth element scandium have been structurally authenticated (six-coordinate Sc^{3+}: effective ionic radius = 0.745 Å).[23−26,28,29] We could access terminal imides of yttrium (d^0, six-coordinate Y^{3+}: 0.900 Å)[29] and lutetium (f^{14}, six-coordinate Lu^{3+}: 0.861 Å)[29] by exploiting the presence of the bulky hydrotris(3-*tert*-butyl-5-methylpyrazolyl)borato ligand (Tp^{tBu,Me}).[27] The applied synthesis protocol involving [Tp^{tBu,Me}LnMe$_2$] as the precursor, however, is limited to the smaller rare-earth metals.[27] Schelter and co-workers isolated the first terminal cerium(IV) imide complex stabilized by a multidentate trianionic ligand (d^{0}f^0, six-coordinate Ce^{4+}: 0.87 Å).[22,29] On the basis of DFT calculations, such anionic ceric imides were assigned a relatively high contribution of covalent bonding compared to trivalent lanthanides.[21,22] Terminal imides of the larger lanthanides with partially filled f orbitals have, to the best of

Received: December 14, 2021
Published: February 25, 2022

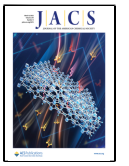

https://doi.org/10.1021/jacs.1c13142
J. Am. Chem. Soc. 2022, 144, 4102−4113

our knowledge, hitherto remained elusive. Herein, we report the Lewis-base-promoted synthesis of terminal imides $[Tp^{tBu,Me}Ln(=NAr^{iPr})(THF)_2]$ (Ln = Ce, Nd, Sm) from trimethylgallium-stabilized rare-earth-metal methylidene precursors (Ln = Ce, Nd, Sm). The successful methylidene protonolysis depends on steric factors and the acidity (pK_a) of the aromatic amine that is used.

RESULTS AND DISCUSSION

Ln(III) Alkylidene Precursors. Drawing on the approach with the highly sterically demanding $Tp^{tBu,Me}$ ancillary ligand, we aimed at further investigating its suitability to stabilize terminal imides of larger Ln(III) centers.[27] Having in mind the ready accessibility of the Lewis-acid-stabilized rare-earth-metal methylidene complex $[Tp^{tBu,Me}La(\mu_3\text{-}CH_2)\{(\mu_2\text{-}Me)\text{-}AlMe_2\}_2]$[30] and the nonavailability of $[Tp^{tBu,Me}LnMe_2]$ for the larger Ln(III), we envisaged a $[Ln{=}CH_2(MMe_3)_2] \rightarrow [Ln{=}NR(Do)_x]$ (M = Al, Ga; Do = donor molecule such as THF) instead of a $[Ln(CH_3)_2] \rightarrow [Ln{=}NR]$ transformation. The feasibility of such a methylidene-based protonolysis under mild conditions was previously demonstrated by Zhou and coworkers using a methylidene-capped trinuclear cluster.[31] Owing to the high nitrogen affinity of aluminum and the likely formation of Lewis-acid-stabilized entities $[Ln{=}NR\text{-}(AlMe_3)]$,[27] we assessed the availability of the respective gallium derivatives. Along these lines, the Ln(III) methylidene complexes $[Tp^{tBu,Me}Ln(\mu_3\text{-}CH_2)\{(\mu_2\text{-}Me)AlMe_2\}_2]$ (**1-Ln**, Ln = Ce, Nd) and $[Tp^{tBu,Me}Ln(\mu_3\text{-}CH_2)\{(\mu_2\text{-}Me)GaMe_2\}_2]$ (**2-Ln**, Ln = La, Ce, Nd, Sm) could be obtained by reacting homoleptic tris(tetramethylgallato) and the tris(tetramethylaluminato) complexes of cerium, neodymium, and samarium with $HTp^{tBu,Me}$ or $KTp^{tBu,Me}$ (Scheme 1).

Scheme 1. Synthesis of Ln(III) Methylidene Precursors $[Tp^{tBu,Me}Ln(\mu_3\text{-}CH_2)\{(\mu_2\text{-}Me)MMe_2\}_2]$ (M = Al (1-Ln), Ga (2-Ln)) via Methane Elimination[a]

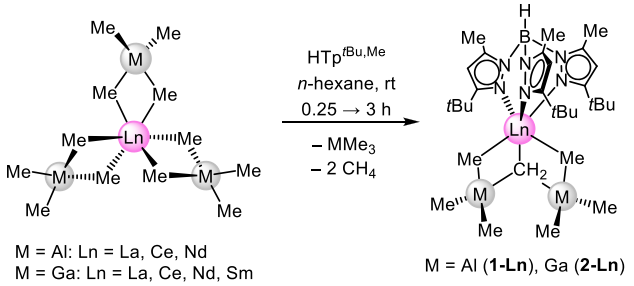

[a]The synthesis of **1-Ce** was conducted with $KTp^{tBu,Me}$ instead of $HTp^{tBu,Me}$, involving $KAlMe_4$ precipitation. (For further information, see the Supporting Information.)

The trimethylgallium-stabilized methylidene complexes **2-Ce** (Supporting Information, Figure S3), **2-Nd**, and **2-Sm** (Figure 1) as well as the trimethylaluminum congeners **1-Ce** and **1-Nd** (Figures S1/S2) are isostructural to the $\{LaAl_2\}$ derivative reported in 2008.[30] Comparing the Ln−C distances of the different lanthanide-methylidene moieties, the lanthanum complex (La−CH_2: 2.519(2) Å)[30] revealed a slightly longer Ln−CH_2 distance than in complexes **1-Ce** (Ce1−C28: 2.484(3) Å), **2-Ce** (Ce1−C25: 2.492(2) Å), **1-Nd** (Nd1−C25: 2.461(2) Å), **2-Nd** (Nd1−C1: 2.450(2) Å), and **2-Sm** (Sm1−C26: 2.414(5) Å). These minor differences are accounted for by the ionic radii of the lanthanide cations

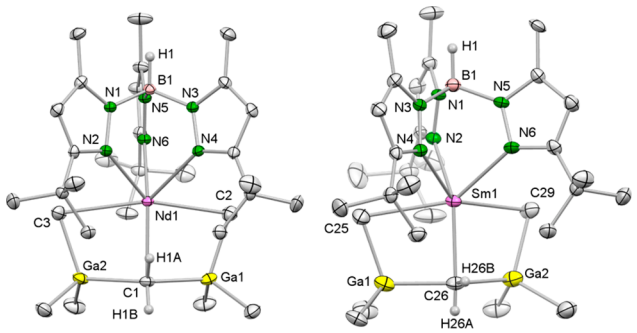

Figure 1. Crystal structures of **2-Nd** (left) and **2-Sm** (right). All atoms are represented by atomic displacement ellipsoids set at 50% probability. Solvent molecules, hydrogen atoms except for those of B−H and CH_2, and the disorder in one of the *tert*-butyl groups are omitted for clarity. Selected interatomic distances (Å) for **2-Nd**: Nd1−C3 2.831(2), Nd1−C1 2.4502(19), and Nd1−C2 2.793(2). Selected interatomic distances (Å) for **2-Sm**: Sm1−C25 2.754(6), Sm1−C26 2.414(5), and Sm1−C29 2.795(5) (Supporting Information).

and are in the expected range.[29] The shorter Nd−CH_2 distance in the case of the trimethylgallium adduct is striking, indicating stronger rare-earth-metal methylidene bonding tantamount to that of the envisaged weaker group 13 Lewis acid stabilization.

As shown in previous NMR studies, the aluminum methyl moieties of the lanthanum congener $[Tp^{tBu,Me}La(\mu_3\text{-}CH_2)\{(\mu_2\text{-}Me)AlMe_2\}_2]$ are highly fluxional,[30] which is also assumed for the paramagnetic cerium, neodymium, and samarium methylidene complexes **2-Ln**. Also, the enhanced mobility of the alkylgallate versus alkylaluminate moieties in solution coupled with a more facile/favorable displacement of the group 13 alkyl[32] should apply to the complexes under study.

$[Ln{=}CH_2(GaMe_3)_2] \rightarrow [Ln{=}NR(THF)_2]$ Transformation. The aromatic amine $[H_2NC_6H_3iPr_2\text{-}2,6]$ (H_2NAr^{iPr}) was previously found to be a convenient imide precursor.[5] Its acidity is suitable for double deprotonation, thus promoting methane elimination from methylidene species as an entropic driving force. In addition, the isopropyl substituents provide favorable steric shielding. Accordingly, methane elimination from compounds **1-Ln** and **2-Ln** was achieved by treatment with 0.9 equiv of H_2NAr^{iPr} under the strict exclusion of donor solvents to afford imide complexes $[Tp^{tBu,Me}Ln(NAr^{iPr})\text{-}(AlMe_3)]$ (**3-Ln**, Ln = Ce, Nd) and $[Tp^{tBu,Me}Ln(NAr^{iPr})\text{-}(GaMe_3)]$ (**4-Ln**, Ln = Nd, Sm) (Scheme 2).

Complexes **3-Ln** and **4-Ln** add to the library of group 13 Lewis-acid-stabilized imide species such as Mindiola's scandium imide complex $[(PNP)Sc(\mu_2\text{-}NAr^{iPr})(\mu_2\text{-}Me)AlMe_2]$ $[PNP{=}N(2\text{-}P\text{-}(CHMe_2)_2\text{-}4\text{-methylphenyl})_2]$[33] or examples from our laboratory including $[Ln_2(\mu_2\text{-}NAr^{iPr})\{(\mu_3\text{-}NAr^{iPr})\text{-}(\mu_2\text{-}Me)_2AlMe\}(AlMe_4)_2]$ (Ln = Y, La, Ce, Nd)[34] and $[Tp^{tBu,Me}Ln(\mu_2\text{-}NR)(\mu_2\text{-}Me)AlMe_2]$ (Ln = Y, R = *t*Bu, Ad, 2,6-$(CH_3)_2C_6H_3$; Ln = Ho, R = *t*Bu, Ad).[27,35] Other bimetallic imides derived from amine deprotonation comprise Xie's mixed amido-imido-ytterbium complex $[Yb(NAr^{iPr})_2(\mu\text{-}NAr^{iPr})Li_2Na(THF)_2]_2$[20] or Schelter's cerium(IV) imides.[21,22] Any attempt to access the putative terminal lanthanum imide from methylidene $[Tp^{tBu,Me}La(\mu_3\text{-}CH_2)\{(\mu_2\text{-}Me)GaMe_2\}_2]$ (**2-La**) failed and led consistently to $[Tp^{tBu,Me}La(HNAr^{iPr})_2]$ (**9-La**).[36] (See Supporting Information Figure S43 for the ^1H NMR spectrum.) Consequently, single deprotonation and the subsequent formation of the bis(anilido) complex is favored over double deprotonation for the largest rare-earth metals

https://doi.org/10.1021/jacs.1c13142
J. Am. Chem. Soc. 2022, 144, 4102−4113

Scheme 2. Synthesis of the Group 13 Methyl-Stabilized Ln(III) Imides [Tp^{tBu,Me}Ln(NC$_6$H$_3$*i*Pr$_2$-2,6)AlMe$_3$] (3-Ln) and [Tp^{tBu,Me}Ln(NC$_6$H$_3$*i*Pr$_2$-2,6)GaMe$_3$] (4-Ln) and the Terminal Ln(III) Imides [Tp^{tBu,Me}Ln(NC$_6$H$_3$*i*Pr$_2$-2,6)(THF)$_2$] (5-Ln) via Methane Elimination from the Corresponding Ln(III) Methylidene Precursors 1-Ln (M = Al) and 2-Ln (M = Ga)[a]

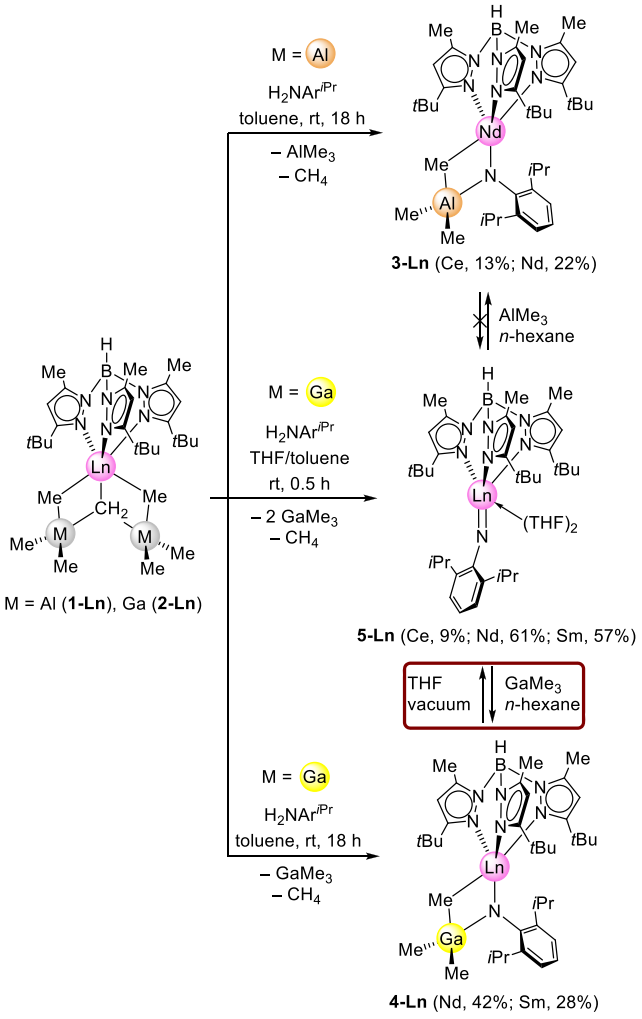

[a]The mutual transformation of **4-Ln** and **5-Ln** occurred by applying either donor addition/vacuum or Lewis acid GaMe$_3$ (Ln = Nd, Sm).

such as lanthanum even though substoichiometric amounts of H$_2$NAr^{iPr} were applied (vide infra).

Being insoluble in aliphatic solvents, **3-Ln** (Ln = Ce, Nd) and **4-Ln** (Ln = Nd, Sm) were crystallized from a saturated toluene/*n*-pentane solution in low to moderate yields. The X-ray diffraction (XRD) analyses revealed isotype compounds that crystallized in the orthorhombic space group *Pnma* (Figure 2). As expected, the Tp^{tBu,Me} ancillary ligand is coordinated to the rare-earth-metal center center in κ^3 fashion (*N*,*N*′,*N*″) with Ln−N(pz) distances in a narrow range (**3-Ce**: 2.566(3)−2.624(3) Å; **3-Nd**: 2.541(6)−2.591(4) Å; **4-Nd**: 2.539(4)−2.594(4) Å; and **4-Sm**: 2.514(5)−2.567(3) Å), similar to the methylidene precursors. Furthermore, the lanthanide center is coordinated by μ_2-bridging imido and methyl functionalities.

Unsurprisingly, the μ_2-bridging methyl groups show significantly elongated Al/Ga−C distances (**3-Ce**: C24−Al1

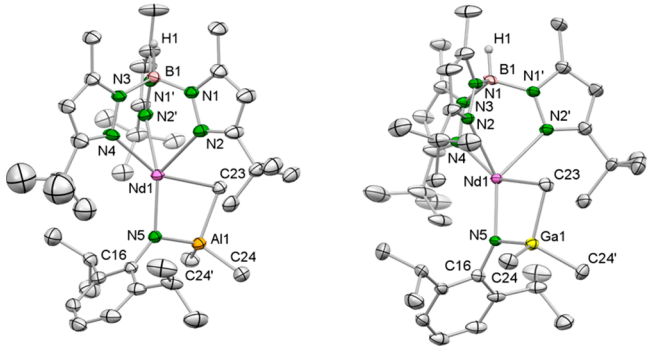

Figure 2. Crystal structures of **3-Nd** (left) and **4-Nd** (right). All atoms are represented by atomic displacement ellipsoids set at 50% probability. Solvent molecules, hydrogen atoms except for those of B−H, and the disorder in one of the *tert*-butyl groups are omitted for clarity. Selected interatomic distances (Å) and angles (deg) for **3-Nd**: Nd1−N5 2.195(5), Nd1−N5−C16 137.3(4), B1−Nd1−N5 174.5(5). Selected interatomic distances (Å) and angles (deg) for **4-Nd**: Nd1−N5 2.158(3), Nd1−N5−C16 141.4(3), and B1−Nd1−N5 172.8(1) (Supporting Information).

2.086(4) Å; **3-Nd**: C23−Al1 2.088(7) Å; **4-Nd**: C23−Ga1 2.106(5) Å; and **4-Sm**: C23−Ga1 2.098(6) Å) compared to the terminal ones (**3-Ce**: C23/23′−Al1 1.985(3) Å; **3-Nd**: C24/24′−Al1 1.990(5) Å; **4-Nd**: C24/24′−Ga1 1.999(3) Å; and **4-Sm**: C24/24′−Ga1 1.989(5) Å). The four-membered metalla-heterocyclic arrangement involving the imido ligand and the group 13 Lewis acid is markedly twisted (**3-Ce**: C24−Ce1−N5 76.27(13)°, Ce1−N5−Al1 101.17(15)°; **3-Nd**: C23−Nd1−N5 77.1(2)°, Nd1−N5−Al1 100.7(2)°; **4-Nd**: C23−Nd1−N5 79.75(13)°, Nd1−N5−Ga1 98.98(13)°; and **4-Sm**: C23−Sm1−N5 80.37(18)°, Sm1−N5−Ga1 98.07(19)°). The Ln−N(imido) distances of 2.213(3) Å (**3-Ce**), 2.195(5) Å (**3-Nd**), 2.158(3) Å (**4-Nd**), and 2.158(4) Å (**4-Sm**) are significantly shorter than the Ln−N distances in complexes with terminal or bridging anilido ligands but are in the range of similar rare-earth-metal imido bonds.[5] Once again, the shorter Nd−N(imido) distances of the trimethylgallium adducts (cf., Nd−C(methylidene) **1-Nd** versus **2-Nd**, vide supra) point to an enhanced multiple-bond character and a weaker interaction of MMe$_3$ across this bond. This is also supported by longer Ln−C distances in the case of the trimethylgallium adducts (**3-Ce**: 2.722(4) Å; **3-Nd**: 2.699(7) Å; **4-Nd**: 2.714(5) Å; and **4-Sm**: 2.655(6) Å). Furthermore, the Ln−N(imido)−C$_{ipso}$ angle is bent as a result of the heterocyclic arrangement (**3-Ce**: 136.2(3)°; **3-Nd**: 137.3(4)°; **4-Nd**: 141.4(3)°; and **4-Sm**: 141.8(4)°).

The Lewis-acid-stabilized imides [Tp^{tBu,Me}Ln(NAr^{iPr})AlMe$_3$] (**3-Ln**) and [Tp^{tBu,Me}Ln(NAr^{iPr})GaMe$_3$] (**4-Ln**) gave intricate NMR spectra, but given the properties of similar Ln(III)-imide complexes, AlMe$_3$ coordination is assumed to be less fluxional than for alkylidenes **1-Ln**. Consequently, the attempted cleavage of trimethylaluminum from compounds **3-Ln** with different donor molecules such as THF, DMAP, and TMEDA (*N*,*N*,*N*′,*N*′-tetramethylethylenediamine) to produce a terminal imide proved infeasible.[27,35,37] The stabilizing group 13 Lewis acid in **3-Ln** is relatively hard according to Pearson's HSAB concept,[38] and interaction with the dianionic imido ligand is considerably stronger than the formation of the THF adduct [AlMe$_3$(THF)].

To verify our working hypothesis that trimethylgallium interacts less strongly with the Ln−N(imido) bond, we reacted

https://doi.org/10.1021/jacs.1c13142
J. Am. Chem. Soc. 2022, 144, 4102−4113

4-Ln with THF (Scheme 2).[27] Eventually, trimethylgallium could be displaced with THF as a donor molecule to afford the terminal imides [$Tp^{tBu,Me}$Ln(=NAr^{iPr})(THF)$_2$] (**5-Ln**, Ln = Ce, Nd, Sm). Concomitantly, the volatile adduct [$GaMe_3$(THF)] formed, which can be removed in vacuo. Alternatively, the terminal Ln(III) imides **5-Ln** can be accessed directly by adding a solution of H_2NAr^{iPr} in THF to a solution of **2-Ln** in toluene. Regarding the crystallized yields of **5-Ln** (**5-Ce**: 9%; **5-Nd**: 61%; and **5-Sm**: 57%), the Ln(III) ionic radii seem to play a major role given that increasing ionic radii appear to favor the single deprotonation of H_2NAr^{iPr} and the formation of bis(anilides) as shown for [$Tp^{tBu,Me}$La(μ_3-CH_2){(μ_2-Me)$GaMe_2$}$_2$] (**2-La**) beforehand (vide supra). The repeatedly obtained poor yield of yellow redox-sensitive **5-Ce** featuring a slightly smaller cerium(III) center can be partially explained by the formation of a red byproduct which unfortunately could not be separated and further identified (Experimental Section). Crucially, the overall marked yield losses for crystalline **5-Ln** can be attributed to several essential recrystallization/purification steps. A likely side product could be [$Me_2GaNHAr^{iPr}$]$_2$, which like its aluminum congener has been obtained previously by refluxing an equimolar mixture of MMe_3 with H_2NAr^{iPr} in toluene overnight.[39] Our reactions did not indicate the formation of [$Me_2GaNHAr^{iPr}$]$_2$ (cf., isolation of [$Tp^{tBu,Me}$Nd($HNAr^{iPr}$)(THF)$_2$][($GaMe_3$)$_2$$NHAr^{iPr}$] (**10-Nd**), vide supra).

Complexes **5-Ln** are insoluble in aliphatic solvents and poorly soluble in aromatic solvents but readily dissolve in THF. Single crystals suitable for XRD analyses were grown from saturated solutions of a THF/toluene/*n*-pentane mixture. The isotype compounds **5-Ln** crystallize in the orthorhombic space group $P2_12_12_1$. The lanthanide center in **5-Ln** is hexacoordinated to three scorpionate nitrogen atoms, the imido ligand, and two THF oxygen atoms (Figure 3).

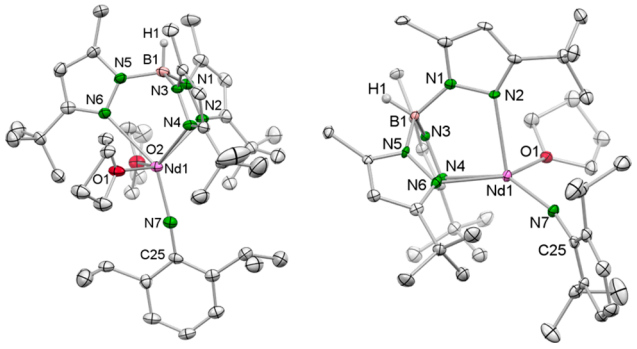

Figure 3. Crystal structures of **5-Ln**, representatively shown for **5-Nd** (left) and **6-Nd** (right). All atoms are represented by atomic displacement ellipsoids set at 50% probability. Hydrogen atoms except for those of B−H as well as the disorder in one THF molecule are omitted for clarity. Selected interatomic distances (Å) and angles (deg) for **5-Nd**: Nd1−N7 2.076(4), Nd1−N7−C25 169.2(4), and B1−Nd1−N7 162.0(2). Selected interatomic distances (Å) and angles (deg) for **6-Nd**: Nd1−N7 2.047(7), Nd1−N7−C25 163.2(6), and B1−Nd1−N7 151.62(2) (Supporting Information).

Moreover, the coordination of the $Tp^{tBu,Me}$ ligand is similar to that in compounds **3-Ln** and **4-Ln** in the routinely observed κ^3 fashion (*N*,*N*′,*N*″) but with slightly elongated Ln−N(pz) distances in the ranges of 2.667(4) to 2.707(4) Å for **5-Ce**, 2.601(4) to 2.674(4) Å for **5-Nd**, and 2.573(5) to 2.657(6) Å for **5-Sm**, reflecting the distinct coordination number.

Compared to other Lewis-base-stabilized terminal rare-earth-metal imides, however,[27] complexes **5-Ln** feature THF as a comparatively weaker donor (cf., DMAP).[23] Note that one crystallization attempt for **5-Nd** in toluene/fluorocyclohexane yielded single crystals of five-coordinate [$Tp^{tBu,Me}$Nd(NAr^{iPr})(THF)] (**6-Nd**, Figure 3). This suggests that the bonding of the first donor molecule to the neodymium center is weak and allows for fluxional behavior in solution. The Ln−N(imido) distances of 2.101(3) Å in **5-Ce** (six-coordinate Ce^{3+}: 1.01 Å), 2.076(4)/av. 2.041 Å in **5-Nd**/**6-Nd** (six-coordinate Nd^{3+}: 0.983 Å), and 2.067(5) Å in **5-Sm** (six-coordinate Sm^{3+}: 0.958 Å) are slightly shorter than in the tetravalent cerium ate complex [(NO_xN)Ce(=$NC_6H_3(CF_3)_2$-3,5)][Cs(2.2.2-crypt)] (2.077(3) Å, NO_xN=N[($CH_2C_6H_4NO$(*t*Bu))]$_3$ (eight-coordinate Ce^{4+}: 0.97 Å)[22] but compare to similar other known trivalent terminal rare-earth-metal imide complexes [$Tp^{tBu,Me}$Y(=NAr)(DMAP)] (**I**, 2.024(4) Å, Ar=$C_6H_3Me_2$-2,6)[27] and [$Tp^{tBu,Me}$Lu(=NAr)(DMAP)] (**II**, 1.993(5) Å, Ar=$NC_6H_3(CF_3)_2$-3,5)[27] considering the differences in the ionic radii and coordination number (Table 1).

Table 1. Comparison of Selected Metrical Parameters in Trivalent Rare-Earth-Metal Imide Complexes

compound	CN	Ln=N_{imido} (Å)	Ln−N_{imido}−C_{ipso} (deg)
3-Ce	5	2.213(3)	76.27(13)
3-Nd	5	2.195(5)	137.3(4)
4-Nd	5	2.158(3)	141.4(3)
4-Sm	5	2.158(4)	141.8(4)
7-Nd	6	2.165(3)	147.6(2)
5 Ce	6	2.101(3)	171.3(3)
5-Nd	6	2.076(4)	169.2(4)
5-Sm	6	2.067(5)	169.3(5)
6-Nd[a]	5	2.047(7)/2.036(7)	163.2(6)/165.8(6)
I[27] (Ln = Y)	5	2.024(4)	173.6(4)
II[27] (Ln = Lu)	5	1.993(5)	175.8(5)
III[26] (Ln = Sc)[b]	5	1.852(4)	168.6(3)

[a]Two molecules in an asymmetric unit. [b]Shortest-known Sc=N_{imido} distance.

Naturally, the respective distances of the terminal imides of the 3d transition metal scandium are shorter, ranging from 1.852(4) to 1.881(5) Å (CN = 5 or 6). The shortest Sc−N(imido) distance of 1.852(4) Å was detected for Chen's THF adduct, five-coordinate [MeC(NAr)CHC(Me)(N-$(CH_2)_2NMe_2$)Sc(=NAr^{iPr})(THF)] (**III**, Table 1).[26] The geometry of six-coordinate complexes **5-Ln** deviates considerably from the ideal octahedral coordination. This is caused by the κ^3 coordination fashion of the ancillary ligand. The almost linear Ln−N(imido)−C_{ipso}(aryl) bond angles Ln1−N7−C25 of 171.3(3)° (**5-Ce**), 169.2(4)°/163.2(6)° (**5-Nd**/**6-Nd**), and 169.3(5)°(**5-Sm**) and the very short Ln−N(imido) distances indicate multiple bond character between the imido nitrogen and the lanthanide centers.

The coordination of the THF donor ligand is labile, enhancing the reactivity of **5-Ln**. The treatment of **5-Ln** with trimethylgallium or trimethylaluminum in aliphatic solvents led to the formation of [$Tp^{tBu,Me}$Ln(NAr^{iPr})($AlMe_3$)] (**3-Ln**) and [$Tp^{tBu,Me}$Ln(NAr^{iPr})($GaMe_3$)] (**4-Ln**), indicating reversibility for the latter reaction. The crucial difference between [Al_2Me_6] and [$GaMe_3$] is the Lewis acidity, which facilitates the isolation of **5-Ln** from **2-Ln** or **4-Ln** in donor solvents. Moreover, the

https://doi.org/10.1021/jacs.1c13142
J. Am. Chem. Soc. 2022, 144, 4102−4113

Scheme 3. Synthesis of Trimethylgallium-Stabilized Neodymium Imide 7-Nd Derived from Sterically Less Demanding 2,4,6-Trimethylaniline, CH-Bond-Activated Neodymium Amide 8-Nd with Sterically More Demanding 2,4,6-Tri-*tert*-butylaniline, and Bis(amido) Neodymium Complex 9-Nd

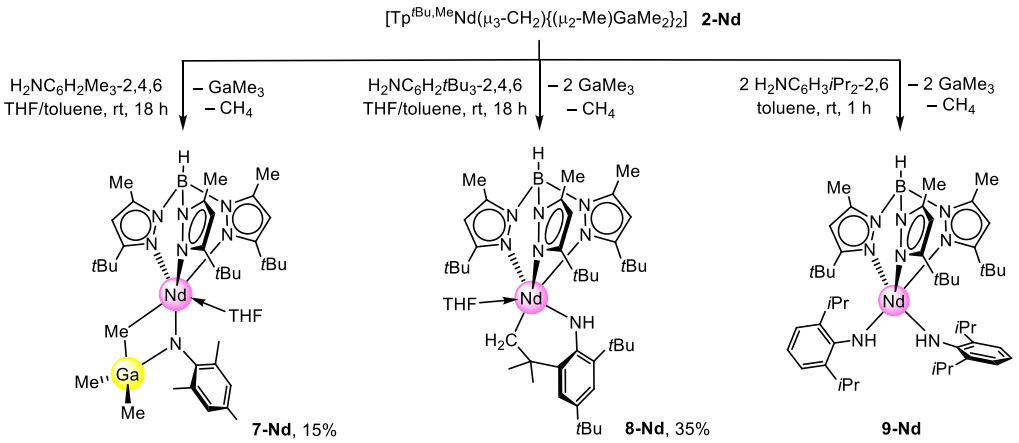

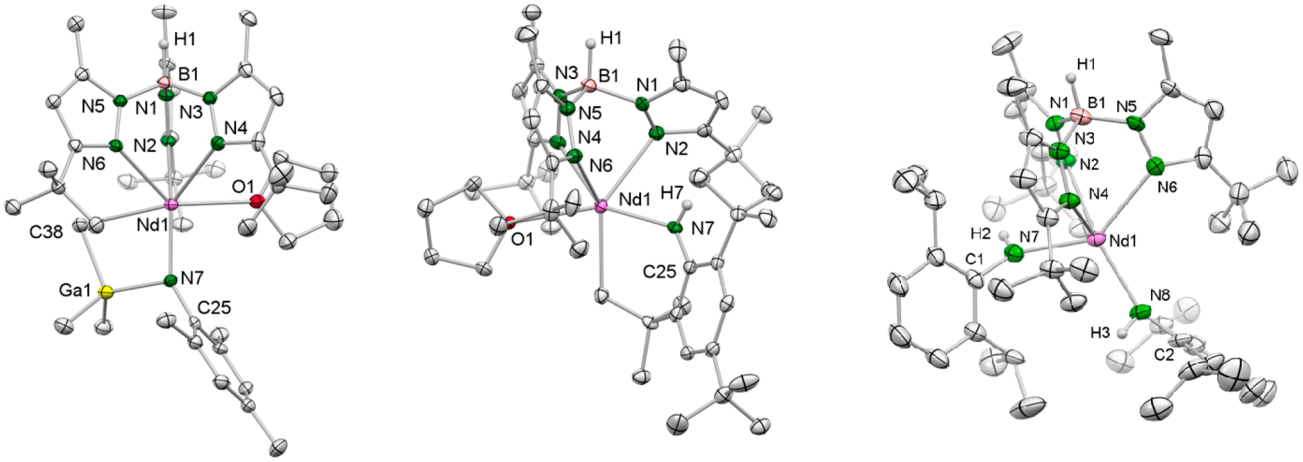

Figure 4. Crystal structures of complexes [Tp^{tBu,Me}Nd(NC$_6$H$_2$Me$_3$-2,4,6)(GaMe$_3$)(THF)] (**7-Nd**), [Tp^{tBu,Me}Nd{NH(C$_6$H$_2$*t*Bu$_2$-2,4-(CMe$_2$CH$_2$)-6)}(THF)] (**8-Nd**), and [Tp^{tBu,Me}Nd(HNAr^{iPr})$_2$] (**9-Nd**) (ellipsoids set to the 50% probability level). Hydrogen atoms except for those of B−H and N−H, the disorder in one *tert*-butyl group and one isopropyl group, and the lattice solvent (three molecules of THF) for **9-Nd** are omitted for clarity. Selected interatomic distances (Å) and angles (deg) for **7-Nd**: Nd1−N7 2.165(3), Nd1−N7−C25 147.6(2), and B1−Nd1−N7 175.74(9). Selected interatomic distances (Å) and angles (deg) for **8-Nd**: Nd1−N7 2.296(4), Nd1−N7−C25 132.2(3), and B1−Nd1−N7 107.4(1). Selected interatomic distances (Å) and angles (deg) for **9-Nd**: Nd1−N7 2.344(5), Nd1−N8 2.312(6), Nd1−N7−C1 153.8(5), and Nd1−N8−C2 144.0(5) (Supporting Information).

reaction is further driven by the formation of the volatile byproduct [GaMe$_3$(THF)].

Role of the Aromatic Amine: Investigations of the Reaction Mechanism. To further assess the role of the primary aromatic amine in the synthesis of such terminal imides, we probed the protonolysis of methylidene complex **2-Nd** with 2,4,6-trimethylaniline (mesidin) and 2,4,6-tri-*tert*-butylaniline (Scheme 3). Remarkably, by using the same protocol as in the synthesis of terminal imide **5-Nd**, the sterically less hindered mesidin afforded complex [Tp^{tBu,Me}Nd(NC$_6$H$_2$Me$_3$-2,4,6)(GaMe$_3$)(THF)] (**7-Nd**, Figure 4/left). Apparently, the unsupported imide is not accessible since the [GaMe$_3$] moiety is more strongly bound, most likely due to a better interaction with the sterically less hindered imido nitrogen. In contrast to five-coordinate [Tp^{tBu,Me}Nd(NAr^{iPr})(GaMe$_3$)] (**4-Nd**), the sterically less encumbered four-membered metalla-heterocyclic arrangement in **7-Nd** gives space for the coordination of a THF molecule. Therefore, the Nd−N(imido) distance of 2.165(3) Å in **7-Nd** is slightly longer than in **4-Nd** (2.158(3) Å). Mechanistically, THF coordination as detected in **7-Nd** represents the initiating step of the [GaMe$_3$] displacement en route to the terminal imide.

On the other hand, the 1:1 reaction of methylidene **2-Nd** with the sterically very demanding 2,4,6-tri-*tert*-butylaniline led to C−H bond activation at one of the *tert*-butyl substituents, thus following a completely different path. This comes to a halt for the metalated complex [Tp^{tBu,Me}Nd{NH(C$_6$H$_2$*t*Bu$_2$-2,4-(CMe$_2$CH$_2$)-6)}(THF)] (**8-Nd**) stage, without a second deprotonation of the amido ligand (Scheme 3, Figure 4/middle). It can be hypothesized that the six-membered heterocycle in **8-Nd** results from σ-bond metathesis of a transiently formed Nd−CH$_3$ (from first protonation) with a [C−H(*t*Bu)] moiety. Mixed methyl/amido complexes such as putative [Tp^{tBu,Me}Nd{N(H)(C$_6$H$_2$*t*Bu$_3$-2,4,6)}(CH$_3$)(THF)] are known precursors or isolable intermediates in rare-earth-metal imide chemistry.[5,35,40] Crucially, although the sterically bulky *tert*-butyl groups cotrigger [GaMe$_3$] displacement, they seem to protect the amido moiety from a second

https://doi.org/10.1021/jacs.1c13142
J. Am. Chem. Soc. 2022, 144, 4102−4113

Scheme 4. Proposed Mechanistic Scenario for the Synthesis of Rare-Earth-Metal Imide Complexes and Competitive Reaction Pathways Involving Aromatic Amines

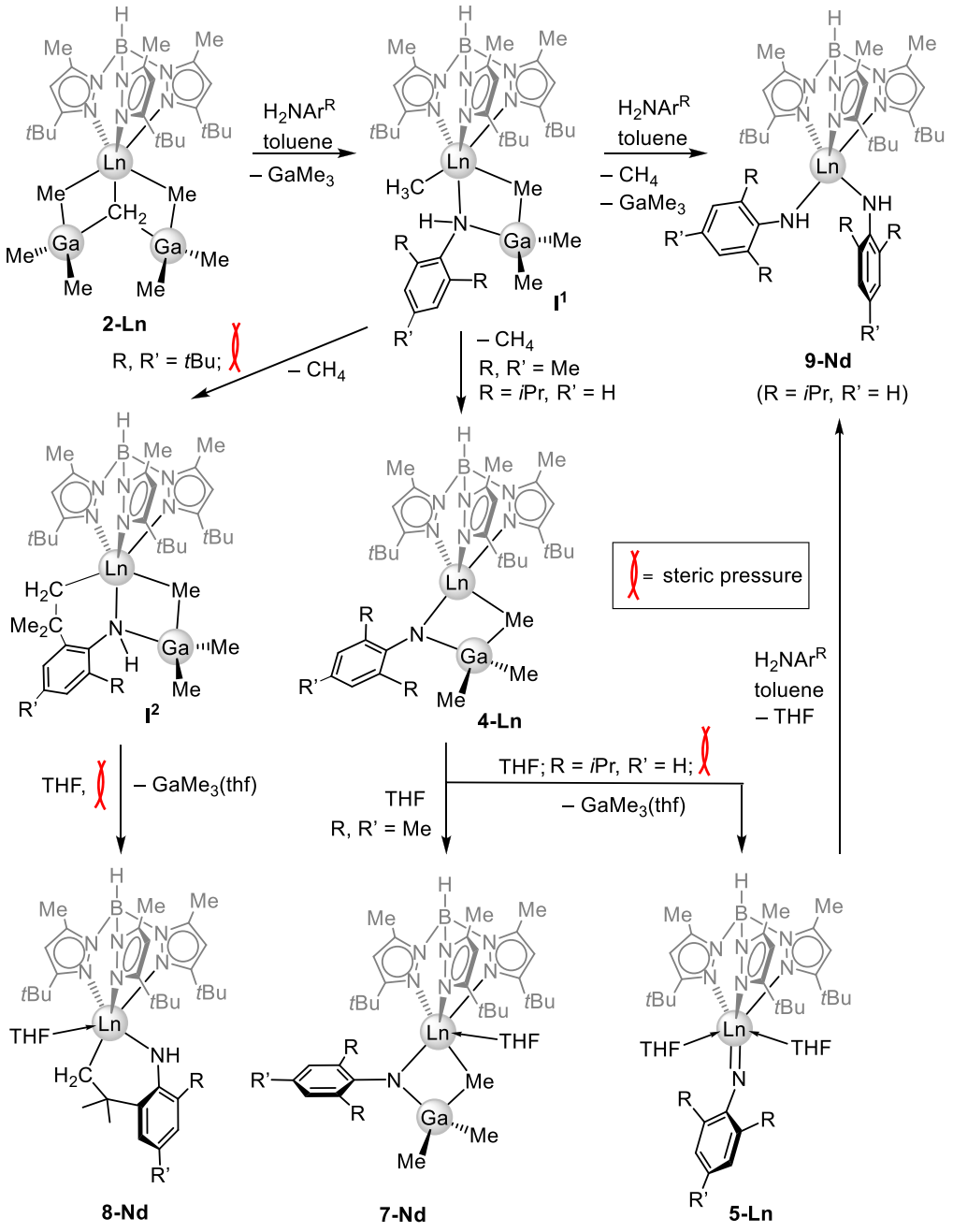

deprotonation, thus being increasingly prone to C–H bond activation. The preferred C–H bond activation of 2,4,6-tri-*tert*-butylaniline in the presence of reactive rare-earth-metal fragments has been evidenced previously.[40] The addition of the [C–H(*t*Bu)] moiety across a transiently formed Nd=NAr^{tBu} imido bond as an alternative pathway toward **8-Nd** seems unlikely on the basis of simple geometrical considerations. Although such hydrocarbyl addition reactions across the Nd=NAr^{R} imido bond have been described for substituents of the ancillary ligand,[3] the involvement of imido backbone substituents R, to the best of our knowledge, has not been observed.

Therefore, the 2,6-substitution pattern of the aromatic amine plays a pivotal role in the formation of a terminal rare-earth-metal imide. The Nd–N(amido) and Nd–C(hydrocarbyl) distances of **8-Nd** amount to 2.296(4) and 2.478(5) Å, respectively, and are therefore in the expected range.

As shown above, the somewhat substoichiometric reaction of **2-Ln** with 2,6-di-*iso*propylaniline afforded **4-Ln** or **5-Ln**. In stark contrast, the 1:2 reaction led to bis(anilido) complex [Tp^{tBu,Me}Nd(HNAr^{iPr})$_2$] (**9-Nd**) (Scheme 3, Figure 4/right). Complex **9-Nd** crystallized in the $P2_12_12_1$ orthorhombic space group and is insoluble in aliphatic solvents. In the solid state, complex **9-Nd** is five-coordinate by the pyrazolyl nitrogen atoms and the amido ligands. The Nd–N(amido) distances of 2.312 and 2.344 Å differ marginally. Nevertheless, both are in the range of similar neodymium anilide compounds.[41] The

https://doi.org/10.1021/jacs.1c13142
J. Am. Chem. Soc. 2022, 144, 4102–4113

bis(amido) formation can be rationalized on the basis that single deprotonation of the aniline is favored. Subsequent second deprotonation of the anilido ligand is impeded because the [Ln−NHAr^{R}] moiety features a proton with lower Brønsted acidity. Thus, in the presence of a second equivalent (or excess) of the amine, the formation of the bis(amido) complex prevails. Alternatively, if the Ln(III) center gets too large, then bis(amido) complex formation is already favored in the presence of substoichiometric amounts of H_2NAr^{iPr}, as shown above for **9-La**. Attempts to utilize the sterically more demanding H_2NAr^{tBu} for the larger La(III) center proved to be futile because no reaction was observed.

A similar reaction has been reported by Mindiola and coworkers showing that the protonolysis of [(PNP)Sc[(μ_3-CH$_2$){(μ_2-Me)(AlMe$_2$)}$_2$] with excess H_2NAr^{iPr} did not produce an imide complex but rather the isolable methyl/amide intermediate [(PNP)Sc(NHAr^{iPr})Me], which reacted further to produce the bis(amido) derivative [(PNP)Sc(NHAr^{iPr})$_2$].[42] Because of the strong donation ability of the amido ligands, the application as precursors for terminal imide complexes is not feasible. In stark contrast, imido exchange reactions and intramolecular amine elimination are widespread methods of preparing titanium or uranium imide complexes, respectively.[43,44] It is worth mentioning that on one occasion the separated ion pair [Tp^{tBu,Me}Nd(HNAr^{iPr})(THF)$_2$]-[(GaMe$_3$)$_2$NHAr^{iPr}] (**10-Nd**) was isolated. (See Figure S17 for the crystal structure.) Crystals of **10-Nd** were obtained from a saturated solution of **2-Nd** and H_2NAr^{iPr} in THF/toluene at low temperature. Apparently, any released [GaMe$_3$]/[(GaMe$_3$)(THF)] in solution negatively affects the formation of terminal imides and therefore must be removed.

A plausible (not exclusive) mechanistic scenario of such Ln(III) arylimide formation sequences is sketched in Scheme 4. The initial step involves the first protonation of the methylidene moiety by the arylamine, generating mixed methyl/amide intermediate **I**^{1} upon the release of one molecule of [GaMe$_3$]. Compounds similar to **I**^{1} have been isolated and structurally characterized in the presence of cyclopentadienyl ancillary ligands.[27,40,45] A second equivalent of the amine affords a bis(amido) complex as shown for **9-Nd**. In the absence of additional amine, the reaction progress is crucially affected by the 2,6-substitution pattern of the arylamine and the size of Ln(III).

Steric pressure as exerted by the *t*Bu substituents of the amido ligand NHAr^{tBu} can trigger σ-bond metathesis with the transiently formed Ln−CH$_3$ to give intermediate **I**^{2}. Again, similar CH(*t*Bu)-bond-activated complexes involving the amido ligand NHAr^{tBu} have been structurally evidenced.[40] Because of a relatively weak interaction of [GaMe$_3$] with the sterically shielded amido nitrogen in **I**^{2}, the gallium alkyl can be easily displaced by the addition of THF to give a metallacyclic donor adduct such as that isolated for **8-Nd**.

To further investigate the formation of neodymium imide **4-Nd** and amide **8-Nd** from methylidene complex **2-Nd** via **I**^{1} and **I**^{2}, we conducted several labeling experiments with D_2NAr^{R} (R = *i*Pr, *t*Bu) at ambient temperature. A low temperature (−80 °C) was used to suppress the rapid exchange of the methyl groups in **2-Nd**, **I**^{1}, and **I**^{2}.[30] The first deuteration of the methylidene moiety by D_2NAr^{R} and concomitant amido ligand formation exhibits the rapid initiating step. Next, methane is eliminated, and in the case of an exclusive reaction of **2-Nd** with D_2NAr^{iPr}, the release of CH_2D_2 should be observed. However, at both ambient temperature and −80 °C only CH_3D could be detected because of rapidly exchanging methyl groups between [GaMe$_3$] and the methylated Nd center. It appears that this methyl group exchange cannot be suppressed at low temperatures and hence is faster than or as fast as the deuteration reaction. The formation of neodymium-bonded deuterated methyl ligands eluded identification as a result of paramagnetic broadening. For the reaction of **2-Nd** with D_2NAr^{tBu}, two different reaction pathways are conceivable: first (pathway I), one of the methyl groups of the ortho-*tert*-butyl substituents of the aromatic amido ligand in **I**^{1} could be activated by a transiently formed Nd−CH_2D or Nd−CH_3 moiety (the latter resulting from the rapid exchange of Nd−CH_2D with [GaMe$_3$]). Such σ-bond metathesis should generate CH_3D or preferentially CH_4 and the metallaheterocycle, while one deuterium would remain on the amido nitrogen. Second (pathway II), as previously mentioned, a transiently formed terminal Nd=N(imido) moiety (involving again initial formation of CH_2D_2 or preferentially CH_3D) could engage in the activation of one of the methyl groups of the ortho-*tert*-butyl substituents, leading to an amido nitrogen bearing a proton instead of a deuterium, and ring closure. Since the experiment at ambient temperate showed the predominant formation of CH_4 and because of the geometrical considerations stated above, reaction path I involving **I**^{1} should mainly apply. Because of otherwise inconclusive NMR experiments with paramagnetic nuclei, we decided to elucidate these reaction pathways only through the detection of gaseous component CH_4 (pathway I) or CH_3D (pathway II). Accordingly, the **2-Nd**/D_2NAr^{tBu} experiment indicated the generation of mainly undeuterated methane CH_4 (Supporting Information), thus favoring pathway I via **I**^{1} and **I**^{2} toward **8-Nd**.

In contrast, sterically less demanding substituents in the 2,6-position of the anilido ligand enable a second deprotonation of anilido ligand NHAr^{R} (R = Me, *i*Pr) via the release of methane and the formation of trimethylgallium-stabilized imide complexes (e.g., **4-Ln**). Such imide formation might be further driven by another proximal [GaMe$_3$] molecule, released during the initiating step. Finally, the interaction of a Lewis base (here THF) with the rare-earth-metal center emerges in the terminal imide upon release of the second [GaMe$_3$] molecule (**5-Ln**) or simply donor coordination to the rare-earth-metal center (**7-Nd**). Crucially, the steric pressure caused by the *i*Pr groups of the imido ligand NHAr^{iPr} seems sufficient to allow for complete [GaMe$_3$] displacement. It should be noted that the Ga−N(imido) distances in **4-Nd** and **7-Nd** are exactly the same (1.992(3) Å).

Finally, bis(amido) complex **9-Nd** could be readily generated via the equimolar reaction of imide **5-Nd** with H_2NAr^{iPr}. The reaction proceeds much more cleanly than when starting out from **2-Ln**. We consider it unlikely that bis(amido) complexes **9-Ln** of the smaller neodymium and samarium are formed in the initial reaction system by applying methylidenes **2-Ln** and slightly substoichiometric amounts of H_2NAr^{iPr}. It seems to be more likely that the imide nitrogen in rapidly formed **4-Ln** is protonated by an additional aromatic amine. This could further weaken [GaMe$_3$] coordination to the neodymium center, which would lead to bis(amido) formation in **9-Ln**. Note that terminal rare-earth-metal imide formation was not observed in the absence of any donor molecule (THF) even though the [GaMe$_3$] molecule is considered to bind weakly to the rare-earth-metal center (as

https://doi.org/10.1021/jacs.1c13142
J. Am. Chem. Soc. 2022, 144, 4102−4113

indicated by rapid methyl group exchange). The formation of bis(amido) complexes **9-Ln** (Ln = Nd, Sm) was not observed in the reactions shown in Scheme 2.

Reactivity of Terminal Imide 5-Nd toward Carbonylic Substrates. Preliminary reactivity tests were conducted with **5-Nd** and benzophenone. NMR-scale reactions showed the feasibility of a $[Nd{=}NR(THF)_2] \rightarrow [Nd{=}O]$ transformation via the generation of *N*-(diphenylmethylene)-2,6-diisopropylaniline. This points to the formation of a molecular neodymium oxide species,[22,42,46] which, however, could not be isolated and further characterized (Supporting Information).

CONCLUSIONS

The $[Ln{=}CH_2(GaMe_3)_2] \rightarrow [Ln{=}NR(THF)_2]$ transformation, utilizing methylidenes $[Tp^{tBu,Me}Ln(\mu_3\text{-}CH_2)\{(\mu_2\text{-}Me)MMe_2\}_2]$ (Ln = Ce, Nd, Sm; M = Al, Ga) and aromatic amines (H_2NAr^R), features a viable approach to synthesizing the first terminal imide complexes of the early "large" lanthanides. However, the successful applicability of such protocols appears to be like walking a tightrope. In fact, one has to draw on a fine balance among the Ln(III) size, the Lewis acidity of the group 13 metal alkyl, the presence of a donor solvent, and the sterics and acidity (pK_a) of the aromatic amine. In particular, it is the comparatively weak interaction of the soft Lewis acid $[GaMe_3]$ with the hard imido nitrogen which facilitates the formation of the unsupported terminal imides. The short Ln−N(imido) distances indicate a very strong bonding/interaction between the Ln(III) centers and the imido nitrogen. The new terminal imido complexes might engage in unprecedented intrinsic imido reactivity (changed ionicity of the Ln=NR bond due to the large Ln(III) size and apparent redox-activity of cerium and samarium), and the partially filled f orbitals might reveal new magneto-optical properties. Moreover, with $[Tp^{tBu,Me}Ln(\mu_3\text{-}CH_2)\{(\mu_2\text{-}Me)MMe_2\}_2]$ in hand, we have a potential Ln−CH_2 synthon for accessing other multiply bonded main group fragments.

EXPERIMENTAL SECTION

General Considerations. *Caution! The group 13 methyl derivatives are highly pyrophoric and react violently when exposed to air and/or moisture.* Therefore, all manipulations were performed under the rigorous exclusion of air and moisture using standard Schlenk, high-vacuum, and glovebox techniques (MB Braun MB200B; <0.1 ppm O_2, <0.1 ppm of H_2O, argon atmosphere). Solvents *n*-hexane, *n*-pentane, diethyl ether, toluene, and tetrahydrofuran (THF) were purified using Grubbs-type columns (MBraun SPS, solvent purification system). Tetrahydrofuran was stored over freshly activated molecular sieves (3 Å). 2,6-Diisopropylaniline (H_2NDipp, 97%, Sigma-Aldrich), 2,4,6-tri-*tert*-butylaniline (99%. Sigma-Aldrich), and 2,4,6-trimethylaniline (98%, Sigma-Aldrich) were dried over CaH_2 and purified by distillation. Benzophenone was purchased from Sigma-Aldrich and used as received. Deuterated 2,6-diisopropylaniline (D_2NDipp) and 2,4,6-tri-*tert*-butylaniline were obtained by stirring the protonated variants with 2 equiv of *n*-BuLi at −78 °C for several hours and subsequent quenching with D_2O and stirring overnight. C_6D_6 (99.6%, Sigma-Aldrich), $[D_8]$THF (99.5%, Euriso-top), and $[D_8]$toluene (99.6%, Sigma-Aldrich) were dried by stirring over Na/K-alloy for at least 24 h and filtered prior to use. All solvents and reagents were stored inside a glovebox. $HTp^{tBu,Me}$ and $KTp^{tBu,Me}$ ($Tp^{tBu,Me}$ = hydrotris(3-*tert*-butyl-5-methylpyrazol)borato) were synthesized by a modification of the published procedure of $HTp^{tBu,Ph}$.[47] $[Ln(AlMe_4)_3]$ and $[Ln(GaMe_4)_3]$ (Ln = Ce, Nd, Sm) were synthesized according to literature procedures.[48,49] The NMR spectra of air- and moisture-sensitive compounds were recorded by using J. Young-valved NMR tubes on a Bruker AVII+400 spectrometer (^{1}H: 400.13 MHz). ^{1}H NMR resonances are referenced to solvent residual resonances and reported in parts per million relative to tetramethylsilane (TMS). Coupling constants are given in Hertz. IR spectra were recorded on a Nicolet 6700 FTIR spectrometer with a DRIFT cell (KBr window), and the samples were prepared in a glovebox and mixed with KBr powder. Alternatively, Nujol oil was used as a carrier material. Elemental analyses were performed on an Elementar Vario Micro Cube.

*$[Tp^{tBu,Me}Ce\{(\mu_3\text{-}CH_2)[(\mu_2\text{-}Me)AlMe_2]_2\}]$ (**1-Ce**).* A suspension of $KTp^{tBu,Me}$ (626 mg, 1.35 mmol) in toluene (3 mL) was added to a solution of $[Ce(AlMe_4)_3]$ (543 mg, 1.35 mmol) in toluene (3 mL). The reaction mixture turned yellow and was stirred for 18 h at ambient temperature. The reaction mixture was dried and extracted several times with cold (−35 °C) toluene, and the extracts were dried again in vacuo to give **1-Ce** as a white powder. Yield: 280 mg, 0.39 mmol, 29%. ^{1}H NMR (400 MHz, C_6D_6): δ 33.53 (s, br), 10.48 (s, br), 5.91 (s, br), −3.87 (s, br), −17.33 (s, br) ppm. $^{11}B\{^1H\}$ NMR (80 MHz, C_6D_6): δ 67.0 (s, br) ppm. IR (KBr): 2965 (s), 2929 (m), 2884 (m), 2819 (w), 2764 (w, B−H), 1543 (s), 1488 (w), 1462 (m), 1427 (s), 1380 (w), 1364 (m), 1346 (s), 1320 (m), 1240 (m), 1180 (s), 1070 (s), 1063 (m), 1021 (m), 1010 (m), 984 (w), 840 (m), 799 (m), 790 (m), 769 (m), 729 (m), 728 (m), 695 (s), 690 (s), 683 (s), 656 (s), 650 (s), 582 (s), 572 (s), 519 (w), 492 (w), 471 (m), 429 (m), cm^{-1}. Elemental analysis (%) calculated for $C_{31}H_{60}Al_2BCeN_6$ (721.75 g mol^{-1}): C 51.59, H 8.38, N 11.64; found: C 51.39, H 8.20, N 11.72.

*$[Tp^{tBu,Me}Nd\{(\mu_3\text{-}CH_2)[(\mu_2\text{-}Me)AlMe_2]_2\}]$ (**1-Nd**).* To a solution of $[Nd(AlMe_4)_3]$ (200 mg, 0.493 mmol) in *n*-hexane (2 mL) a solution of $HTp^{tBu,Me}$ (209 mg, 0.493 mmol) in *n*-hexane (2 mL) was slowly added. The pale-green solution was stirred at ambient temperature for 4 h. A pale-green solid precipitated, which was filtered off and washed twice with *n*-hexane. The solid was dried under reduced pressure. Green crystals of **1-Nd** could be harvested at −35 °C in toluene. Yield: 167 mg, 0.230 mmol, 47%. ^{1}H NMR (500 MHz, $CDCl_3$, 26 °C): δ 33.41 (s, br), 10.80 (s, br), 6.08 (s, br), −20.25 (s, br) ppm. IR (Nujol, $\tilde{\nu}$): 2583 (m, B−H), 1538 (s), 1460 (vs, Nujol), 1378 (s, Nujol), 1347 (s), 1326 (m), 1243 (w), 1174 (s), 1124 (w), 1072 (m), 1021 (w), 984 (w), 850 (w), 793 (m), 778 (m), 695 (s), 664 (m), 591 (m), 514 (w) cm^{-1}. Elemental analysis (%) calculated for $C_{31}H_{60}Al_2BN_6Nd$ (725.88 g/mol): C 51.30, H 8.33, N 11.58; found: C 51.02, H 8.11, N 11.31.

*$[Tp^{tBu,Me}Ce\{(\mu_3\text{-}CH_2)[(\mu_2\text{-}Me)GaMe_2]_2\}]$ (**2-Ce**).* A cold (−35 °C) solution of $HTp^{tBu,Me}$ (188 mg, 0.44 mmol) in toluene (3 mL) was added to a cold (−35 °C) solution of $[Ce(GaMe_4)_3]$ (235 mg, 0.44 mmol) in toluene (3 mL). The reaction mixture was stirred for 1 h at ambient temperature. A white precipitate had formed after several hours when the mixture was stored at −35 °C. The white precipitate was washed with cold *n*-hexane to yield **2-Ce** as a white powder. Yield: 284 mg, 0.35 mmol, 80%. ^{1}H NMR (400 MHz, C_6D_6): δ 10.88 (s, br), 6.04 (s, br), −4.62 (s, br), −17.85 (s, br) ppm. $^{11}B\{^1H\}$ NMR (80 MHz, C_6D_6): δ 64.6 (s, br) ppm. IR (KBr): 2964 (s), 2931 (m), 2861 (m), 2768 (w), 2578 (w, B−H), 1544 (s), 1489 (w), 1462 (m), 1429 (s), 1381 (w), 1363 (m), 1348 (s), 1318 (m); 1241(w), 1200 (m), 1188 (m), 1176 (s), 1071 (m), 1063 (m), 1022 (w), 1011 (w), 984 (w), 877 (w), 808 (m), 789 (m), 769 (m), 729 (m), 702 (m), 679 (m), 654 (m), 639 (m), 601 (w), 536 (m), 508 (s), 436 (m), 428 (m), 421 (m) cm^{-1}. Elemental analysis (%) calculated for $C_{31}H_{60}BCeGa_2N_6$ (807.24 g mol^{-1}): C 46.13, H 7.49, N 10.41; found: C 46.16, H 7.22, N 10.45.

*$[Tp^{tBu,Me}Nd\{(\mu_3\text{-}CH_2)[(\mu_2\text{-}Me)GaMe_2]_2\}]$ (**2-Nd**).* To a solution of $[Nd(GaMe_4)_3]$ (147 mg, 0.275 mmol) in *n*-hexane (2 mL) a solution of $HTp^{tBu,Me}$ (117 mg, 0.275 mmol) in *n*-hexane (2 mL) was added slowly. Immediate gas evolution occurred, and the blue solution turned pale blue. The solution was stirred at ambient temperature for 15 min. A pale-blue solid precipitated, which was filtered off and washed twice with *n*-hexane. The solid was dried under reduced pressure. Single crystals of **2-Nd** suitable for XRD analysis were obtained from a concentrated solution in toluene. Yield: 128 mg, 0.158 mmol, 57%. ^{1}H NMR (400 MHz, C_6D_6, 26 °C): δ 35.93 (s, br),

https://doi.org/10.1021/jacs.1c13142
J. Am. Chem. Soc. 2022, 144, 4102−4113

11.62 (s, br), 3.72 (s, br), −21.49 (s, br) ppm. $^{11}B\{^1H\}$ NMR (96 MHz, C_6D_6, 26 °C): δ 73.1 (s, br) ppm. DRIFT ($\tilde{\nu}$): 2964 (vs), 2930 (m), 2864 (w), 2775 (w), 2543 (w, B−H), 1543 (s), 1462 (w), 1429 (s), 1362 (w), 1348 (m), 1203 (w), 1176 (s), 1069 (m), 1023 (w), 798 (m), 702(w), 646 (w), 640 (w), 512 (s), 430 (m) cm^{-1}. Elemental analysis (%) calculated for $C_{31}H_{60}BGa_2N_6Nd$ (811.36 g/mol): C 45.89, H 7.45, N 10.36; found: C 45.94, H 7.45, N 10.47.

*[Tp^{tBu,Me}Sm{(μ_3-CH$_2$)[(μ_2-Me)GaMe$_2$]$_2$}] (**2-Sm**).* Following the procedure described for **2-Nd**, [Sm(GaMe$_4$)$_3$] (329 mg, 0.609 mmol) in *n*-hexane (4 mL) and a solution of HTp^{tBu,Me} (259 mg, 0.609 mmol) in *n*-hexane (5 mL) were stirred for 3 h at ambient temperature, affording **2-Sm** as an orange solid. Yield: 424 mg, 0.517 mmol, 85%. Single crystals suitable for XRD analysis formed from a mixed solution of toluene and *n*-pentane. ^1H NMR (400 MHz, C_6D_6, 26 °C): δ 5.36 (s, br), 1.87 (s, br), −4.20 (s, br), −9.35 (s, br) ppm. $^{11}B\{^1H\}$ NMR (96 MHz, C_6D_6, 26 °C): δ 6.3 (s, br) ppm. DRIFT ($\tilde{\nu}$): 2965 (vs), 2862 (w), 2784 (vw), 2544 (vw, B−H), 1543 (vs), 1489 (w), 1463 (m), 1431 (vs), 1379 (vw), 1350 (m), 1325 (w), 1242 (w), 1204 (m), 1187 (s), 1120 (vw), 1069 (w), 1023 (w), 1012 (w), 981 (w), 875 (w), 856 (vw), 843 (vw), 798 (s), 790 (s), 772 (s), 729 (s), 705 (vs), 647 (s), 580 (m), 532 (vs), 513 (vs), 499 (m), 471 (w), 435 (s), 420 (vs), 414 (s) cm^{-1}. Elemental analysis (%) calculated for $C_{31}H_{60}BGa_2N_6Nd$ (817.48 g/mol): C 45.55, H 7.40, N 10.28; found: C 46.08, H 7.32, N 9.95.

*[Tp^{tBu,Me}Ce(NC$_6$H$_3$*i*Pr$_2$-2,6)(AlMe$_3$)] (**3-Ce**).* A solution of [KHNC$_6$H$_3$*i*Pr$_2$-2,6] (42 mg, 0.19 mmol) in toluene (3 mL) was added to a solution of **1-Ce** (140 mg, 0.19 mmol) in toluene (3 mL). The reaction mixture was stirred for 18 h at ambient temperature. Crystallization at −35 °C in THF yielded **3-Ce** as yellow crystals. Yield: 20 mg, 0.02 mmol, 13%. ^1H NMR (400 MHz, THF-d_8): δ 6.77 (s, br), 5.66 (s, br), 2.04 (s, br), 1.17 (s, br), −1.17 (s, br), −1.44 (s, br) ppm. Elemental analysis (%) calculated for $C_{39}H_{66}AlBCeN_7$ (810.91 g/mol): C 57.77, H 8.20, N 12.09; found: C 58.32, H 8.18, N 11.56.

*[Tp^{tBu,Me}Nd(NC$_6$H$_3$*i*Pr$_2$-2,6)(AlMe$_3$)] (**3-Nd**).* A solution of [H$_2$NC$_6$H$_3$*i*Pr$_2$-2,6] (29.7 mg, 0.138 mmol) in 3 mL of toluene was added to a solution of **1-Nd** (100 mg, 0.138 mmol) in 3 mL of toluene and stirred for 18 h. The solution was concentrated, and after several days at −35 °C, green single crystals of **3-Nd** suitable for XRD analysis were obtained. Crystallized yield: 25.0 mg, 0.0307 mmol, 22%. ^1H NMR (400 MHz, C_6D_6, 26 °C): δ 27.48 (s, br), 16.98 (s, br), 10.64 (s, br), 5.98 (s, br), −12.82 (s, br), −20.00 (s, br), −34.14 (s, br) ppm. $^{11}B\{^1H\}$ NMR (96 MHz, C_6D_6, 26 °C): δ 66.4 (s, br) ppm. DRIFT ($\tilde{\nu}$): 2965 (m), 2931 (w), 2577 (vw, B−H), 1585 (vw), 1543 (s), 1491 (vw), 1460 (w), 1426 (s), 1380 (vw), 1346 (m), 1323 (w), 1241 (w), 1231 (w), 1184 (s), 1104 (vw), 1067 (m), 1022 (w), 1010 (w), 985 (vw), 928 (vw), 884 (vw), 858 (w), 843 (w), 801 (m), 788 (s), 769 (w), 761 (w), 697 (vs), 647 (s), 647 (s), 619 (m), 588 (m), 558 (w), 520 (vw), 495 (w), 470 (w), 439 (w), 423 (w) cm^{-1}. Elemental analysis (%) calculated for $C_{39}H_{66}AlBN_7Nd$ (815.04 g/mol): C 57.82, H 8.09, N 11.55; found: C 58.22, H 8.03, N 11.47.

*[Tp^{tBu,Me}Nd(NC$_6$H$_3$*i*Pr$_2$-2,6)(GaMe$_3$)] (**4-Nd**).* [H$_2$NC$_6$H$_3$*i*Pr$_2$-2,6] (29.5 mg, 0.166 mmol) in 3 mL of toluene was added to a solution of **2-Nd** (150 mg, 0.185 mmol) in 3 mL of toluene and stirred for 18 h. The solution was concentrated, and after several days at −35 °C, pale-green single crystals of **4-Nd** suitable for XRD analysis had formed. Yield: 67.0 mg, 0.0781 mmol, 42%. ^1H NMR (400 MHz, C_6D_6, 26 °C): δ 31.88 (s, br), 29.53 (s, br), 27.48 (s, br), 19.19 (s, br), 16.79 (s, br), 11.34 (s, br), −8.20 (s, br), −12.89 (s, br), −34.08 (s, br), −35.78 (s, br) ppm. $^{11}B\{^1H\}$ NMR (96 MHz, C_6D_6, 26 °C): δ 183.8 (s, br) ppm. DRIFT ($\tilde{\nu}$): 3037 (vw), 2963 (vs), 2929 (m), 2863 (w), 2579 (vw, B−H), 1584 (vw), 1543 (vs), 1493 (vw), 1460 (w), 1428 (s), 1416 (s), 1379 (w), 1352 (s), 1342 (m), 1325 (w), 1306 (w), 1229 (m), 1241 (m), 1187 (vs), 1180 (vs), 1146 (vw), 1106 (w), 1093 (vw), 1066 (m), 1038 (vw), 1021 (w), 1010 (w), 985 (w), 931 (vw), 886 (w), 860 (vw), 846 (vw), 802 (w), 796 (m), 788 (s), 768 (s), 760 (vs), 728 (w), 693 (w), 677 (m), 647 (w), 618 (w), 602 (m), 566 (vw), 535 (w), 524 (w), 478 (w), 439 (w), 418 (m), 404 (m) cm^{-1}. Elemental analysis (%) calculated for $C_{39}H_{66}BGaN_7Nd$ (857.78 g/mol): C 54.61, H 7.76, N 11.43; found: C 54.66, H 7.50, N 11.49.

*[Tp^{tBu,Me}Sm(NC$_6$H$_3$*i*Pr$_2$-2,6)(GaMe$_3$)] (**4-Sm**).* Following the procedure described for **4-Nd**, **2-Sm** (100 mg, 0.122 mmol) in toluene (3 mL) and a solution of [H$_2$NC$_6$H$_3$*i*Pr$_2$-2,6] (21.7 mg, 0.122 mmol) in toluene (3 mL) afforded **4-Sm** as a red solid. Yield: 28 mg, 0.034 mmol, 28%. Single crystals suitable for XRD analysis formed from a mixed solution of toluene and *n*-pentane. ^1H NMR (400 MHz, C_6D_6, 26 °C): δ 12.07 (s, br), 6.62 (s, br), 4.81 (s, br), 3.96 (s, br), 2.42 (s, br), −0.78 (s, br), −2.79 (s, br), −3.26 (s, br) ppm. $^{11}B\{^1H\}$ NMR (96 MHz, C_6D_6, 26 °C): δ −0.9 (s, br) ppm. DRIFT ($\tilde{\nu}$): 3037 (vw), 2964 (vs), 2927 (m), 2863 (w), 2580 (vw, B−H), 1584 (vw), 1543 (vs), 1494 (w), 1460 (m), 1418 (s), 1379 (w), 1379 (w), 1352 (m), 1325 (w), 1306 (w), 1242 (s), 1229 (m), 1188 (vs), 1179 (vs), 1146 (vw), 1106 (w), 1067 (m), 1038 (vw), 1021 (w), 1010 (w), 985 (w), 886 (w), 860 (m), 802 (w), 788 (s), 771 (s), 760 (s), 728 (w), 694 (w), 681 (w), 647 (m), 601 (w), 568 (vw), 534 (w), 522 (w), 476 (w), 438 (m), 419 (m), 407 (s) cm^{-1}. Elemental analysis (%) calculated for $C_{39}H_{66}BGaN_7Nd$ (863.90 g/mol): C 54.22, H 7.70, N 11.35; found: C 54.38, H 8.04, N 10.82.

*[Tp^{tBu,Me}Ce(NC$_6$H$_3$*i*Pr$_2$-2,6)(THF)$_2$] (**5-Ce**).* A solution of [H$_2$NC$_6$H$_3$*i*Pr$_2$-2,6] (36 mg, 0.2 mmol) in THF (3 mL) was added to a solution of **2-Ce** (136 mg, 0.16 mmol) in toluene (3 mL). The resulting solution turned from yellow to red, and was stirred for 18 h at ambient temperature. Crystallization at −35 °C in THF yielded **5-Ce** as yellow crystals and amorphous, unidentified, red side products. Yield: 13 mg, 0.01 mmol, 9%. ^1H NMR (400 MHz, THF-d_8): δ 10.13 (s, br), 4.66 (s, br), 3.48 (s, br), 1.94 (s, br), 1.41 (s, br), −0.28 (s, br), −9.39 (s, br) ppm. Elemental analysis (%) calculated for $C_{44}H_{73}BCeN_7O_2$ (883.04 g mol^{-1}): C 59.85, H 8.33, N 11.10; found: C 59.77, H 8.25, N 10.98.

*[Tp^{tBu,Me}Nd(NC$_6$H$_3$*i*Pr$_2$-2,6)(THF)$_2$] (**5-Nd**).* Compound **2-Nd** (200 mg, 0.246 mmol) was dissolved in 3 mL of toluene. A solution of [H$_2$NC$_6$H$_3$*i*Pr$_2$-2,6] (39.2 mg, 0.221 mmol) in 3 mL of THF was added slowly, and the reaction mixture was stirred for 30 min. The solution was concentrated, and after several days at −35 °C, green crystals had formed. Compound **5-Nd** was recrystallized several times. Yield: 132 mg, 0.149 mmol, 61%. ^1H NMR (400 MHz, [D$_8$]THF, 26 °C): δ 38.66 (s, br), 23.12 (s, br), 11.71 (s, br), 8.15 (s, br), −32.86 (s, br) ppm. $^{11}B\{^1H\}$ NMR (96 MHz, C_6D_6, 26 °C): δ 147.4 (s, br) ppm. DRIFT ($\tilde{\nu}$): 2959 (vs), 2860 (w), 2559 (vw, B−H), 1580 (w), 1543 (vw), 1486 (m), 1460 (m), 1423 (m), 1396 (s), 1350 (m), 1317 (vs), 1203 (m), 1180 (s), 1136 (w), 1102 (vw), 1067 (s), 1030 (m), 1011 (w), 986 (w), 896 (s), 870 (w), 845 (w), 792 (m), 782 (m), 763 (w), 728 (m), 707 (vw), 669 (vw), 647 (m), 585 (vw), 513 (vw), 440 (vw) cm^{-1}. Elemental analysis (%) calculated for $C_{44}H_{73}BN_7NdO_2$ (887.17 g/mol): C 59.57, H 8.29, N 11.05; found: C 59.35, H 8.38, N 10.72.

*[Tp^{tBu,Me}Sm(NC$_6$H$_3$*i*Pr$_2$-2,6)(THF)$_2$] (**5-Sm**).* Following the procedure described for **5-Nd**, using **2-Sm** (212 mg, 0.259 mmol) in toluene (4 mL) and a solution of [H$_2$NC$_6$H$_3$*i*Pr$_2$-2,6] (46.0 mg, 0.259 mmol) in THF (4 mL) afforded **5-Sm** as a dark-red solid. The compound was recrystallized several times. Yield: 131 mg, 0.147 mmol, 57%. Single crystals suitable for XRD analysis formed from a mixed solution of THF and *n*-hexane. ^1H NMR (400 MHz, C_6D_6, 26 °C): δ 5.91 (s, br), 5.17 (s, br), 4.73 (s, br), 4.23 (s, br), 1.87 (s, br), 1.13 (s, br), −3.16 (s, br), −5.56 (s, br) ppm. $^{11}B\{^1H\}$ NMR (96 MHz, C_6D_6, 26 °C): δ 11.3 (s, br) ppm. DRIFT ($\tilde{\nu}$): 2962 (vs), 2861 (w), 2561 (vw, B−H), 1580 (w), 1543 (vs), 1487 (vw), 1458 (m), 1419 (s), 1397 (s), 1350 (s), 1320 (vs), 1257 (vs), 1202 (s), 1179 (vs), 1137 (w), 1103 (vw), 1068 (vs), 1028 (m), 1012 (w), 986 (w), 897 (m), 869 (w), 846 (w), 792 (m), 784 (s), 766 (m), 729 (w), 708 (w), 669 (w), 647 (s), 600 (vw), 586 (vw), 518 (vw), 472 (vw), 441 (m), 418 (vw) cm^{-1}. Elemental analysis (%) calculated for $BN_7C_{44}H_{73}O_2Sm$ (893.29 g/mol): C 59.16, H 8.24, N 10.98; found: C 59.19, H 7.79, N 10.95.

*[Tp^{tBu,Me}Nd(NC$_6$H$_3$Me$_3$-2,4,6)(GaMe$_3$)(THF)] (**7-Nd**).* Following the procedure described for **5-Nd**, using **2-Nd** (158 mg, 0.195 mmol) in toluene (3 mL) and a solution of [H$_2$NC$_6$H$_3$Me$_3$-2,4,6] (26.3 mg, 0.195 mmol) in THF (2 mL) afforded **7-Nd** as a green solid. Yield:

https://doi.org/10.1021/jacs.1c13142
J. Am. Chem. Soc. 2022, 144, 4102−4113

27.3 mg, 0.0297 mmol, 15%. Single crystals suitable for XRD analysis formed from a toluene solution. ^{1}H NMR (400 MHz, C_6D_6, 26 °C): δ 26.62 (s, br), 15.70 (s, br), 14.84 (s, br), 11.72 (s, br), −17.18 (s, br), −32.76 (s, br), −38.34 (s, br), ppm. ^{11}B{^{1}H} NMR (96 MHz, C_6D_6, 26 °C): δ −0.3 (s, br) ppm. Multiple attempts to obtain a satisfactory microanalysis failed.

*[Tp^{tBu,Me}Nd{HN(C$_6$H$_2$tBu$_2$-2,4-(CMe$_2$CH$_2$)-6}(THF)] (**8-Nd**).* Following the procedure described for **5-Nd**, using **2-Nd** (55.3 mg, 0.0681 mmol) in toluene (3 mL) and a solution of [H$_2$NC$_6$H$_3$tBu$_3$-2,4,6] (17.8 mg, 0.0681 mmol) in THF (2 mL) afforded **8-Nd** as a green solid. Yield: 21.4 mg, 0.0238 mmol, 35%. Single crystals suitable for XRD analysis formed from a toluene solution. ^{1}H NMR (400 MHz, C_6D_6, 26 °C): δ 24.18 (s, br), 12.64 (s, br), 11.64 (s, br) ppm. ^{11}B{^{1}H} NMR (96 MHz, C_6D_6, 26 °C): δ −5.0 (s, br) ppm. Elemental analysis (%) calculated for $GaC_{42}H_{74}BN_7NdO$ (899.22 g/mol): C 61.44, H 8.63, N 10.90; found: C 61.18, H 8.44, N 9.25.

*[Tp^{tBu,Me}La(HNC$_6$H$_3$iPr$_2$-2,6)$_2$] (**9-La**).* In a J. Young-valved tube, to a solution of [H$_2$NC$_6$H$_3$iPr$_2$-2,6] (5.3 mg, 0.0299 mmol) in 0.2 mL of C_6D_6 a solution of [Tp^{tBu,Me}La{(μ_3-CH$_2$)[(μ_2-Me)GaMe$_2$]$_2$}] (24.1 mg, 0.0299 mmol) in 0.2 mL of C_6D_6 was added. ^{1}H NMR (400 MHz, C_6D_6, 26 °C): δ 7.94 (d, 4H, $^3J_{HH}$ 6.72 Hz, *m*-ArH), 6.84 (t, 2H, $^3J_{HH}$ 15.47 Hz, *p*-ArH), 5.60 (s, 3H, pz-*H*), 5.00 (s, 2H, N*H*), 3.19 (m, 4H, *i*Pr-C*H*), 1.94 (s, 9H, pz-CH_3), 1.28 (s, 27H, pz-C(CH_3)$_3$), 1.24 (d, 24H, $^3J_{HH}$ 6.80 Hz, *i*Pr-CH_3) ppm.

*[Tp^{tBu,Me}Nd(HNC$_6$H$_3$iPr$_2$-2,6)$_2$] (**9-Nd**).* Method (a): To a solution of [H$_2$NC$_6$H$_3$iPr$_2$-2,6] (92.9 mg, 0.524 mmol) in 3 mL of toluene a solution of **2-Nd** (170 mg, 0.201 mmol) in 3 mL of toluene was added and stirred for 1 h. The concentrated solution was stored at −35 °C, and after several days, green crystals had formed, which were analyzed by XRD as **9-Nd**. Method (b): To a solution of **5-Nd** (19.4 mg, 0.0217 mmol) in 3 mL of toluene a solution of [H$_2$NC$_6$H$_3$iPr$_2$-2,6] (3.87 mg, 0.0217 mmol) in 3 mL of toluene was added. The color changed from green to blue immediately. Afterward the solvent was removed under vacuum. ^{1}H NMR (400 MHz, C_6D_6, 26 °C): δ 14.03 (s, br), 9.06 (s, br), 3.17 (s, br), 1.85 (s, br), 13.00 (s, br) ppm. Elemental analysis (%) calculated for $C_{48}H_{76}BN_8Nd$ (920.24 g/mol): C 62.65, H 8.32, N 12.18; found: C 62.71, H 8.30, N 12.13.

*[Tp^{tBu,Me}Nd(HNC$_6$H$_3$iPr$_2$-2,6)$_2$][(GaMe$_3$)$_2$(HNC$_6$H$_3$iPr$_2$-2,6)] (**10-Nd**).* To a solution of [H$_2$NC$_6$H$_3$iPr$_2$-2,6] (39.3 mg, 0.222 mmol) in 3 mL of THF a solution of [Tp^{tBu,Me}Nd{(μ_3-CH$_2$)[(μ_2-Me)-GaMe$_2$]$_2$}] (200 mg, 0.246 mmol) in 3 mL of toluene was added and stirred for 18 h. After several days at −35 °C, a few green crystals were obtained, which were analyzed by XRD as **10-Nd**.

[Ph$_2$C═N(C$_6$H$_3$iPr$_2$-2,6)]. In a J. Young-valved tube, to a solution of [Tp^{tBu,Me}Nd(NC$_6$H$_3$iPr$_2$-2,6)(THF)$_2$] (**5-Nd**) (3.8 mg, 0.00428 mmol) in 0.2 mL of C_6D_6 a solution of benzophenone (0.78 mg, 0.00428 mmol) in 0.2 mL of C_6D_6 was added. ^{1}H NMR (400 MHz, C_6D_6, 26 °C): δ 7.95 (d, 2H, $^3J_{HH}$ 6.91 Hz), 7.10−6.99 (m, 6H), 6.94−6.83 (m, 4H), 3.06 (m, 2H, *i*Pr-C*H*), 1.23 (d, 6H, $^3J_{HH}$ 6.77 Hz, *i*Pr-CH_3), 0.98 (d, 6H, $^3J_{HH}$ 6.74 Hz, *i*Pr-CH_3) ppm; signals are given only for imine *N*-(diphenylmethylene)-2,6-diisopropylaniline.

Labeling Studies. In a J. Young-valved tube, to a solution of **2-Nd** (R = *i*Pr: 7.2 mg, 0.00893 mmol; R = *t*Bu: 8.3 mg, 0.0102 mmol) in 0.4 mL of C_6D_6 a solution of D_2NAr^R (R = *i*Pr: 1.6 mg, 0.00893 mmol, 0.2 mL C_6D_6; R = *t*Bu: 2.7 mg, 0.0102 mmol, 0.2 mL [D_8]THF) was added at ambient temperature. Low-temperature experiments were started by adding the aromatic amine solution to a solution of **2-Nd** in [D_8]toluene, precooled to −80 °C.

■ ASSOCIATED CONTENT

Supporting Information

The Supporting Information is available free of charge at https://pubs.acs.org/doi/10.1021/jacs.1c13142.

Supporting figures, detailed crystallographic data, and spectroscopic data (NMR) (PDF)

Accession Codes

CCDC 2125445−2125461 contain the supplementary crystallographic data for this paper. These data can be obtained free of charge via www.ccdc.cam.ac.uk/data_request/cif, or by emailing data_request@ccdc.cam.ac.uk, or by contacting The Cambridge Crystallographic Data Centre, 12 Union Road, Cambridge CB2 1EZ, UK; fax: +44 1223 336033.

■ AUTHOR INFORMATION

Corresponding Author

Reiner Anwander − *Institut für Anorganische Chemie, Eberhard Karls Universität Tübingen, 72076 Tübingen, Germany;* orcid.org/0000-0002-1543-3787; Email: reiner.anwander@uni-tuebingen.de

Authors

Theresa E. Rieser − *Institut für Anorganische Chemie, Eberhard Karls Universität Tübingen, 72076 Tübingen, Germany*

Renita Thim-Spöring − *Institut für Anorganische Chemie, Eberhard Karls Universität Tübingen, 72076 Tübingen, Germany*

Dorothea Schädle − *Institut für Anorganische Chemie, Eberhard Karls Universität Tübingen, 72076 Tübingen, Germany*

Peter Sirsch − *Institut für Anorganische Chemie, Eberhard Karls Universität Tübingen, 72076 Tübingen, Germany*

Rannveig Litlabø − *Department of Chemistry, University of Bergen, N-5007 Bergen, Norway*

Karl W. Törnroos − *Department of Chemistry, University of Bergen, N-5007 Bergen, Norway;* orcid.org/0000-0001-6140-5915

Cäcilia Maichle-Mössmer − *Institut für Anorganische Chemie, Eberhard Karls Universität Tübingen, 72076 Tübingen, Germany;* orcid.org/0000-0001-7638-1610

Complete contact information is available at: https://pubs.acs.org/10.1021/jacs.1c13142

Notes

The authors declare no competing financial interest.

■ ACKNOWLEDGMENTS

Dedicated to Prof. Dr. Kazushi Mashima on the occasion of his 65th birthday. We gratefully acknowledge support from the German Science Foundation (grant: AN 238/15-2).

■ REFERENCES

(1) Giesbrecht, G. R.; Gordon, J. C. Lanthanide alkylidene and imido complexes. *Dalton Trans.* **2004**, 2387−2393.

(2) Summerscales, O. T.; Gordon, J. C. Complexes containing multiple bonding interactions between lanthanoid elements and main-group fragments. *RSC Advance* **2013**, *3*, 6682−6692.

(3) Lu, E.; Chu, J.; Chen, Y. Scandium Terminal Imido Chemistry. *Acc. Chem. Res.* **2018**, *51*, 557−566.

(4) Zhu, Q.; Zhu, J.; Zhu, C. Recent progress in the chemistry of lanthanide-ligand multiple bonds. *Tetrahedron Lett.* **2018**, *59*, 514−520.

(5) Schädle, D.; Anwander, R. Rare-earth metal and actinide organoimide chemistry. *Chem. Soc. Rev.* **2019**, *48*, 5752−5805.

(6) Pedersen, S. F.; Schrock, R. R. Multiple metal-carbon bonds. 27. Preparation of tungsten(VI) phenylimido alkyl and alkylidene complexes. *J. Am. Chem. Soc.* **1982**, *104*, 7483−7491.

(7) (a) Mountford, P. New titanium imido chemistry *Chem. Commun.* **1997**, 2127−2134. (b) Hazari, N.; Mountford, P. Reactions and Applications of Titanium Imido Complexes. *Acc. Chem. Res.* **2005**, *38*, 839−849.

(8) Duncan, A. P.; Bergman, R. G. Selective transformations of organic compounds by imidozirconocene complexes. *Chem. Rec.* **2002**, *2*, 431−445.
(9) (a) Mindiola, D. J. Oxidatively Induced Abstraction Reactions. A Synthetic Approach to Low-Coordinate and Reactive Early Transition Metal Complexes Containing Metal−Ligand Multiple Bonds. *Acc. Chem. Res.* **2006**, *39*, 813−821. (b) Fout, A. R.; Kilgore, U. J.; Mindiola, D. J. The Progression of Synthetic Strategies to Assemble Titanium Complexes Bearing the Terminal Imide Group. *Chem.—Eur. J.* **2007**, *13*, 9428−9440.
(10) Nomura, K.; Zhang, W. (Imido)vanadium(v)-alkyl, -alkylidene complexes exhibiting unique reactivity towards olefins and alcohols. *Chem. Sci.* **2010**, *1*, 161−173.
(11) Kawakita, K.; Parker, B. F.; Kakiuchi, Y.; Tsurugi, H.; Mashima, K.; Arnold, J.; Tonks, I. A. Reactivity of terminal imido complexes of group 4−6 metals: Stoichiometric and catalytic reactions involving cycloaddition with unsaturated organic molecules. *Coord. Chem. Rev.* **2020**, *407*, 213118.
(12) Grünwald, A.; Anjana, S. S.; Munz, D. Terminal Imido Complexes of the Groups 9−11: Electronic Structure and Developments in the Last Decade. *Eur. J. Inorg. Chem.* **2021**, *2021*, 4147−4166.
(13) For examples, see (a) Dietrich, H. M.; Törnroos, K. W.; Anwander, R. Ionic Carbenes": Synthesis, Structural Characterization, and Reactivity of Rare-Earth Metal Methylidene Complexes. *J. Am. Chem. Soc.* **2006**, *128*, 9298−9299. (b) Gerber, L. C. H.; Le Roux, E.; Törnroos, K. W.; Anwander, R. Elusive Trimethyllanthanum: Snapshots of Extensive Methyl Group Degradation in La·Al Heterobimetallic Complexes. *Chem.—Eur. J.* **2008**, *14*, 9555−9564. (c) Zhang, W.-X.; Wang, Z.; Nishiura, M.; Xi, Z.; Hou, Z. $Ln_4(CH_2)_4$ Cubane-Type Rare-Earth Methylidene Complexes Consisting of "$(C_5Me_4SiMe_3)LnCH_2$" Units (Ln = Tm, Lu). *J. Am. Chem. Soc.* **2011**, *133*, 5712−5715. (d) Li, S.; Wang, M.; Liu, B.; Li, L.; Cheng, J.; Wu, C.; Liu, D.; Liu, J.; Cui, D. Lutetium-Methanediide-Alkyl Complexes: Synthesis and Chemistry. *Chem.—Eur. J.* **2014**, *20*, 15493−15498. (e) Li, T.; Zhang, G.; Guo, J.; Wang, S.; Leng, X.; Chen, Y. Tris(pyrazolyl)methanide Complexes of Trivalent Rare-Earth Metals. *Organometallics* **2016**, *35*, 1565−1572.
(14) Kratsch, J.; Roesky, P. W. Rare-Earth-Metal Methylidene Complexes. *Angew. Chem., Int. Ed.* **2014**, *53*, 376−383.
(15) (a) Trifonov, A. A.; Bochkarev, M. N.; Schumann, H.; Loebel, J. Reduction of Azobenzene by Naphthaleneytterbium: A Tetranuclear Ytterbium(III) Complex Combining 1,2-Diphenylhydrazido(2−) and Phenylimido Ligands. *Angew. Chem., Int. Ed.* **1991**, *30*, 1149−1151. (b) Cui, D.; Tardif, O.; Hou, Z. Tetranuclear Rare Earth Metal Polyhydrido Complexes Composed of "$(C_5Me_4SiMe_3)LnH_2$" Units. Unique Reactivities toward Unsaturated C−C, C−N, and C−O Bonds. *J. Am. Chem. Soc.* **2004**, *126*, 1312−1313. (c) Berthet, J.-C.; Thuéry, P.; Ephritikhine, M. Polyimido Clusters of Neodymium and Uranium, Including a Cluster with an $M_6(\mu_3\text{-}N)_8$ Core. *Eur. J. Inorg. Chem.* **2008**, *2008*, 5455−5459.
(16) Anwander, R. Self-Assembly" in Organolanthanide Chemistry: Formation of Rings and Clusters. *Angew. Chem., Int. Ed.* **1998**, *37*, 599−602.
(17) Strongly polarized Al−N imido bonds and associated high reactivity also frustrate the isolation of terminal aluminum imides: (a) Li, J.; Li, X.; Huang, W.; Hu, H.; Zhang, J.; Cui, C. Synthesis, Structure, and Reactivity of a Monomeric Iminoalane. *Chem.—Eur. J.* **2012**, *18*, 15263−15266. (b) Anker, M. D.; Schwamm, R. J.; Coles, M. P. Synthesis and reactivity of a terminal aluminium−imide bond. *Chem. Commun.* **2020**, *56*, 2288−2291.
(18) Evans, W. J.; Ansari, M. A.; Ziller, J. W.; Khan, S. I. Utility of Arylamido Ligands in Yttrium and Lanthanide Chemistry. *Inorg. Chem.* **1996**, *35*, 5435−5444.
(19) Gordon, J. C.; Giesbrecht, G. R.; Clark, D. L.; Hay, P. J.; Keogh, D. W.; Poli, R.; Scott, B. L.; Watkin, J. G. The First Example of a μ_2-Imido Functionality Bound to a Lanthanide Metal Center: X-ray Crystal Structure and DFT Study of $[(\mu\text{-ArN})Sm(\mu\text{-NHAr})(\mu\text{-Me})AlMe_2]_2$ (Ar = 2,6-$iPr_2C_6H_3$). *Organometallics* **2002**, *21*, 4726−4734.
(20) Chan, H.-S.; Li, H.-W.; Xie, Z. Synthesis and structural characterization of imido−lanthanide complexes with a metal−nitrogen multiple bond. *Chem. Commun.* **2002**, 652−653.
(21) Solola, L. A.; Zabula, A. V.; Dorfner, W. L.; Manor, B. C.; Carroll, P. J.; Schelter, E. J. An Alkali Metal-Capped Cerium(IV) Imido Complex. *J. Am. Chem. Soc.* **2016**, *138*, 6928−6931.
(22) (a) Solola, L. A.; Zabula, A. V.; Dorfner, W. L.; Manor, B. C.; Carroll, P. J.; Schelter, E. J. Cerium(IV) Imido Complexes: Structural, Computational, and Reactivity Studies. *J. Am. Chem. Soc.* **2017**, *139*, 2435−2442. (b) Cheisson, T.; Kersey, K. D.; Mahieu, N.; McSkimming, A.; Gau, M. R.; Carroll, P. J.; Schelter, E. J. Multiple Bonding in Lanthanides and Actinides: Direct Comparison of Covalency in Thorium(IV)- and Cerium(IV)-Imido Complexes. *J. Am. Chem. Soc.* **2019**, *141*, 9185−9190.
(23) Lu, E.; Li, Y.; Chen, Y. A scandium terminal imido complex: synthesis, structure and DFT studies. *Chem. Commun.* **2010**, *46*, 4469−4471.
(24) Lu, E.; Chu, J.; Chen, Y.; Borzov, M. V.; Li, G. Scandium terminal imido complex induced C−H bond selenation and formation of an Sc−Se bond. *Chem. Commun.* **2011**, *47*, 743−745.
(25) Rong, W.; Cheng, J.; Mou, Z.; Xie, H.; Cui, D. Facile Preparation of a Scandium Terminal Imido Complex Supported by a Phosphazene Ligand. *Organometallics* **2013**, *32*, 5523−5529.
(26) Chu, J.; Han, X.; Kefalidis, C. E.; Zhou, J.; Maron, L.; Leng, X.; Chen, Y. Lewis Acid Triggered Reactivity of a Lewis Base Stabilized Scandium-Terminal Imido Complex: C−H Bond Activation, Cycloaddition, and Dehydrofluorination. *J. Am. Chem. Soc.* **2014**, *136*, 10894−10897.
(27) Schädle, D.; Meermann-Zimmermann, M.; Schädle, C.; Maichle-Mössmer, C.; Anwander, R. Rare-Earth Metal Complexes with Terminal Imido Ligands. *Eur. J. Inorg. Chem.* **2015**, *2015*, 1334−1339.
(28) Patrick, E. A.; Yang, Y.; Piers, W. E.; Maron, L.; Gelfand, B. S. A monoanionic pentadentate ligand platform for scandium−pnictogen multiple bonds. *Chem. Commun.* **2021**, *57*, 8640−8643.
(29) Shannon, R. D. Revised effective ionic radii and systematic studies of interatomic distances in halides and chalcogenides. *Acta Crystallogr., Sect. A* **1976**, *32*, 751−767.
(30) Litlabø, R.; Zimmermann, M.; Saliu, K.; Takats, J.; Törnroos, K. W.; Anwander, R. A Rare-Earth Metal Variant of the Tebbe Reagent. *Angew. Chem., Int. Ed.* **2008**, *47*, 9560−9564.
(31) Hong, J.; Zhang, L.; Wang, K.; Zhang, Y.; Weng, L.; Zhou, X. Methylidene Rare-Earth-Metal Complex Mediated Transformations of C-N, N-N and N-H Bonds: New Routes to Imido Rare-Earth-Metal Clusters. *Chem.—Eur. J.* **2013**, *19*, 7865−7873.
(32) Zimmermann, M.; Litlabø, R.; Törnroos, K. W.; Anwander, R. "Metastable" $Lu(GaMe_4)_3$ Reacts Like Masked $[LuMe_3]$: Synthesis of an Unsolvated Lanthanide Dimethyl Complex. *Organometallics* **2009**, *28*, 6646−6649.
(33) Scott, J.; Basuli, F.; Fout, A. R.; Huffman, J. C.; Mindiola, D. J. Evidence for the Existence of a Terminal Imidoscandium Compound: Intermolecular C-H Activation and Complexation Reactions with the Transient Sc-NAr Species. *Angew. Chem., Int. Ed.* **2008**, *47*, 8502−8505.
(34) Schädle, D.; Schädle, C.; Schneider, D.; Maichle-Mössmer, C.; Anwander, R. Versatile $Ln_2(\mu\text{-}NR)_2$-Imide Platforms for Ligand Exchange and Isoprene Polymerization. *Organometallics* **2015**, *34*, 4994−5008.
(35) Schädle, D.; Maichle-Mössmer, C.; Schädle, C.; Anwander, R. Rare-Earth-Metal Methyl, Amide, and Imide Complexes Supported by a Superbulky Scorpionate Ligand. *Chem.—Eur. J.* **2015**, *21*, 662−670.
(36) Recent attempts to isolate a related terminal [La═PR] phosphinidene were frustrated by ancillary backbone activation: Watt, F. A.; McCabe, K. N.; Schoch, R.; Maron, L.; Hohloch, S. A transient lanthanum phosphinidene complex. *Chem. Commun.* **2020**, *56*, 15410−15413.

https://doi.org/10.1021/jacs.1c13142
J. Am. Chem. Soc. 2022, 144, 4102−4113

(37) Schädle, C.; Schädle, D.; Eichele, K.; Anwander, R. Methylaluminum-Supported Rare-Earth-Metal Dihydrides. *Angew. Chem., Int. Ed.* **2013**, *52*, 13238−13242.
(38) Pearson, R. G. Hard and Soft Acids and Bases. *J. Am. Chem. Soc.* **1963**, *85*, 3533−3539.
(39) Waggoner, K. M.; Power, P. P. Reactions of Trimethylaluminum and Trimethylgallium with Bulky Primary Amines: Structural Characterization of the Thermolysis Products. *J. Am. Chem. Soc.* **1991**, *113*, 3385−3393.
(40) Schädle, D.; Enders, M.; Schädle, C.; Maichle-Mössmer, C.; Törnroos, K. W.; Anwander, R. Reactivity of halfsandwich rare-earth metal methylaluminates toward potassium (2,4,6-tri-tert-butylphenyl)amide and 1-adamantylamine. *New J. Chem.* **2015**, *39*, 7640−7648.
(41) (a) Li, W.; Xue, M.; Xu, F.; Tu, J.; Zhang, Y.; Shen, Q. Synthesis, characterization of bridged bis(amidinate) lanthanide amides and their application as catalysts for addition of amines to nitriles for monosubstituted N-arylamidines. *Dalton Trans.* **2012**, *41*, 8252−8260. (b) Liu, C.; Qian, Q.; Nie, K.; Wang, Y.; Shen, Q.; Yuan, D.; Yao, Y. Lanthanide anilido complexes: synthesis, characterization, and use as highly efficient catalysts for hydrophosphonylation of aldehydes and unactivated ketones. *Dalton Trans.* **2014**, *43*, 8355−8362.
(42) Scott, J.; Fan, H.; Wicker, B. F.; Fout, A. R.; Baik, M.-H.; Mindiola, D. J. Lewis Acid Stabilized Methylidene and Oxoscandium Complexes. *J. Am. Chem. Soc.* **2008**, *130*, 14438−14439.
(43) Hayton, T. W.; Boncella, J. M.; Scott, B. L.; Palmer, P. D.; Batista, E. R.; Hay, P. J. Synthesis of Imido Analogs of the Uranyl Ion. *Science* **2005**, *310*, 1941−1943.
(44) Schwarz, A. D.; Nielson, A. J.; Kaltsoyannis, N.; Mountford, P. The first group 4 metal bis(imido) and tris(imido) complexes. *Chem. Sci.* **2012**, *3*, 819−824.
(45) Thim, R.; Dietrich, H. M.; Bonath, M.; Maichle-Mössmer, C.; Anwander, R. Pentamethylcyclopentadienyl-Supported Rare-Earth-Metal Benzyl, Amide, and Imide Complexes. *Organometallics* **2018**, *37*, 2769−2777.
(46) Schädle, D.; Meermann-Zimmermann, M.; Maichle-Mössmer, C.; Schädle, C.; Törnroos, K. W.; Anwander, R. Rare-earth metal methylidene complexes with $Ln_3(\mu_3\text{-}CH_2)(\mu_3\text{-}Me)(\mu_2\text{-}Me)_3$ core structure. *Dalton Trans.* **2015**, *44*, 18101−18110.
(47) Kisko, J. L.; Hascall, T.; Kimblin, C.; Parkin, G. Phenyl tris(3-*tert*-butylpyrazolyl)borato complexes of lithium and thallium, [PhTpBu]M (M = Li, Tl): a novel structure for a monomeric tris(pyrazolyl)boratothallium complex and a study of its stereochemical nonrigidity by ^{1}H and ^{205}Tl NMR spectroscopy. *J. Chem. Soc., Dalton Trans.* **1999**, 1929−1936.
(48) Zimmermann, M.; Frøystein, N. Å.; Fischbach, A.; Sirsch, P.; Dietrich, H. M.; Törnroos, K. W.; Herdtweck, E.; Anwander, R. Homoleptic Rare-Earth Metal(III) Tetramethylaluminates: Structural Chemistry, Reactivity, and Performance in Isoprene Polymerization. *Chem.—Eur. J.* **2007**, *13*, 8784−8800.
(49) Evans, W. J.; Anwander, R.; Doedens, R. J.; Ziller, J. W. The Use of Heterometallic Bridging Moieties To Generate Tractable Lanthanide Complexes of Small Ligands. *Angew. Chem., Int. Ed. Engl.* **1994**, *33*, 1641−1644.

https://doi.org/10.1021/jacs.1c13142
J. Am. Chem. Soc. 2022, 144, 4102−4113